

VILNIUS UNIVERSITY  
CENTER FOR PHYSICAL SCIENCES AND TECHNOLOGY

KĘSTUTIS STEPONKEVIČIUS

**THIRD HARMONIC GENERATION AND SIX-WAVE MIXING  
OF FEMTOSECOND LASER PULSES IN AIR**

Summary of doctoral dissertation  
Physical sciences, Physics (02P)

Vilnius, 2016

The research was performed in 2012–2016 at Vilnius University Laser Research Center.

**Scientific supervisor** – dr. Virgilijus Vaičaitis (Vilnius University, Physical sciences, Physics - 02P).

**Doctoral committee:**

**Chairman** – prof. habil. dr. Valdas Sirutkaitis (Vilnius university, physical sciences, physics - 02P).

**Members:**

dr. Ramūnas Adomavičius (Center for Physical Sciences and Technology, Physical sciences, Physics – 02P),

dr. Rimantas Grigonis (Vilnius university, physical sciences, physics – 02P),

dr. Viačeslav Kudriašov (Vilnius university, physical sciences, physics – 02P),

dr. Audrius Pugžlys (Vienna university of technology, physical sciences, physics – 02P).

The dissertation will be defended under open consideration in the Council of Physics on the 23th of September, 2016, 3 p.m. at the Laser Research Center of Vilnius University, room 306, Saulėtekio ave. 10, Vilnius, Lithuania.

The summary of the dissertation was distributed on the 23th of August, 2016.

The dissertation is available at Vilnius University, Center for Physical Sciences and Technology libraries, and VU website: [www.vu.lt/naujienos/ivykiu-kalendorius](http://www.vu.lt/naujienos/ivykiu-kalendorius).

VILNIAUS UNIVERSITETAS  
FIZINIŲ IR TECHNOLOGIJOS MOKSLŲ CENTRAS

KĘSTUTIS STEPONKEVIČIUS

**FEMTOSEKUNDINIŲ LAZERIO IMPULSŲ  
TREČIOSIOS HARMONIKOS GENERAVIMAS IR  
ŠEŠIABANGIS DAŽNIŲ MAIŠYMAS ORE**

Daktaro disertacijos santrauka  
Fiziniai mokslai, fizika (02P)

Vilnius, 2016 metai

Disertacija rengta 2012–2016 metais Vilniaus universitete Lazerinių tyrimų centre.

**Mokslinis vadovas** – dr. Virgilijus Vaičaitis (Vilniaus universitetas, fiziniai mokslai, fizika – 02P).

**Disertacija ginama Vilniaus universiteto Fizikos mokslo krypties taryboje:**

**Pirmininkas** – prof. habil. dr. Valdas Sirutkaitis (Vilniaus universitetas, fiziniai mokslai, fizika – 02P).

**Nariai:**

dr. Ramūnas Adomavičius (Fizinių ir technologijos mokslų centras, fiziniai mokslai, fizika – 02P),

dr. Rimantas Grigonis (Vilniaus universitetas, fiziniai mokslai, fizika – 02P),

dr. Viačeslav Kudriašov (Vilniaus universitetas, fiziniai mokslai, fizika – 02P),

dr. Audrius Pugžlys (Vienos technikos universitetas, fiziniai mokslai, fizika – 02P).

Disertacija bus ginama viešame Fizikos mokslo krypties tarybos posėdyje 2016 m. rugsėjo 23 d. 15:00 val. Vilniaus universiteto lazerinių tyrimų centro 306 auditorijoje, Saulėtekio al. 10, Vilniuje, Lietuvoje.

Disertacijos santrauka išsiuntinėta 2016 m. rugpjūčio mėn. 23 d.

Disertaciją galima peržiūrėti Vilniaus universiteto, Fizinių ir technologijos mokslų centro bibliotekose ir VU interneto svetainėje adresu: [www.vu.lt/naujienos/ivykiu-kalendorius](http://www.vu.lt/naujienos/ivykiu-kalendorius).

# CONTENTS

<b>Introduction</b>	<b>6</b>
<b>1. Third harmonic generation in air</b>	<b>14</b>
1.1. Experimental methods . . . . .	14
1.2. Spatial, spectral and energy characteristics of third harmonic generation . . . . .	15
1.3. Spectral shifts of third harmonic radiation and refocusing of femtosecond laser pulses . . . . .	18
<b>2. Noncollinear six-wave mixing in air</b>	<b>23</b>
2.1. Experimental methods . . . . .	23
2.2. Spatial, spectral and energy characteristics of noncollinear six-wave mixing . . . . .	24
<b>3. Applications of noncollinear six-wave mixing for temporal characterization of femtosecond laser pulses</b>	<b>31</b>
<b>Conclusions</b>	<b>36</b>
<b>Bibliography</b>	<b>38</b>
<b>Santrauka</b>	<b>47</b>
<b>Curriculum vitae</b>	<b>48</b>

## INTRODUCTION

Optical harmonic generation is a well-established technique to produce coherent radiation in spectral regions, where conventional lasers are not available [1-4]. In particular, third-order-harmonic generation (THG) in gaseous media is a source of coherent radiation in the ultraviolet (UV) and vacuum ultraviolet (VUV) [5-11]. THG can find applications not only for the efficient frequency tripling over a wide range of wavelengths, but also in a variety of scientific and technological areas including the atmospheric pollutants detection through third harmonic (TH) induced-fluorescence [2], laser-induced plasma diagnostic [12], ultrafast spectroscopy of atoms and molecules [13], time-resolved and high-resolution biological imaging [14] and supercontinuum generation [15, 16].

Unfortunately, the phase-matching conditions of THG can not be satisfied in a medium of normal dispersion such as gases. Moreover, in the tight-focusing limit the TH wave generated prior the focus interferes destructively with TH wave generated beyond focus [17]. Also, when femtosecond laser pulses are focused, the other nonlinear effects, for example, optical kerr effect, plasma generation [18], conical radiation [19-22], four-wave mixing [23-32], etc. [33-36], compete with THG. Thus, the self-focusing and plasma electron defocusing lead to the femtosecond laser pulse filamentation in air [37-41] and the intensity clamping [42, 43]. Therefore the light peak intensity usually is limited to about  $10^{13}$  W/cm<sup>2</sup> during pulse propagation in air [44-46]. Moreover, during laser-induced filamentation in air a two-color filament can be formed and then the central and conical part of TH are generated [1, 2, 4]. This two-color filamentation effect is due to an intensity-dependent nonlinear phase-locking between the fundamental harmonic (FH) and the TH pulses, which could extend the THG phase-matching condition over the longer propagation distances [1, 2, 4, 49, 50]. In two-color filament the clamped laser intensity is sufficient for the THG [1-4] and the achieved efficiency of TH generated by infrared (IR) femtosecond laser pulses in air is about 0.2 percent [47, 48]. Moreover, when the filament is formed and the intensity clamping takes place, the losses due to the ionization process may be low, therefore later, when the defocusing starts, the self-focusing due to nonlinear Kerr effect may be repeated. This process is

called refocusing. As a result, the filament line is not uniform [51, 52]. However, during the femtosecond laser filamentation in air the spectra of TH and FH pulses are broadened due to electron plasma generation [53-59], self-phase modulation (SPM) [60, 61], cross-phase modulation (XPM) [62, 63] and the temporal self-steepening [64-66].

Thus, unfortunately, the physical mechanisms of the THG during femtosecond filamentation in gases are not fully understood and the complicated spatial and spectral structure of TH strongly limit the number of potential applications of a UV light source [67-71]. This motivated us to study the spectral and spatial properties of the FH and TH generated in air by focused femtosecond laser pulses of variable energy. In contrast to other papers [1, 2] for the experiments we have used lenses of longer focal length (1–2 m) which allowed us to increase the spectral shifts of TH. Moreover, we were motivated to investigate the influence of refocusing to the enhanced spectral shifts of FH and TH.

On the other hand, the higher-order nonlinear polarization terms induced in a medium by intense femtosecond laser pulses may become comparable to or larger than the lower-order ones [72-76]. However, recently a series of reports on TH enhancement by use of additional laser beams have been published [77-81]. Although such increase of THG efficiency has been explained mainly by the influence of laser-induced gas plasma, a full theoretical model of THG by a few laser beams still needs to be developed. This motivated us to study the role of quintic optical nonlinearity during frequency tripling of femtosecond laser pulses in air, when five laser photons are mixed together to create a TH photon. We have chosen a noncollinear two-beam pump configuration because this method allows one to control phase-matching conditions of nonlinear interaction via a simple change of the beam crossing angle. In contrast to previous reports, where two crossed beams were also used for THG [72-76], this research was performed at very small laser-beam crossing angles, since our preliminary plane-wave analysis revealed that only within this region (at about 10 mrad) phase-matching conditions could be satisfied for the noncollinear six-wave mixing (SWM) in air.

## **MAIN OBJECTIVE**

The main objective of this thesis is to investigate the TH spectral shifts and their changes due to the refocusing and to demonstrate the THG due to the noncollinear SWM by

analyzing the characteristics (spatial, spectral and energy) and the application opportunities of this nonlinear effect by using femtosecond laser pulses in air.

## **THE TASKS OF THE THESIS**

1. To investigate the spatial, spectral and energy characteristics of THG in air by using femtosecond laser pulses.
2. To study evolution of the FH as well as TH pulses and spectra during their propagation in the filament. Also, to investigate the influence of refocusing of femtosecond laser pulses in air on THG and on the spectral shifts of the FH and TH.
3. To demonstrate THG through SWM in a medium of normal dispersion (air) by using the femtosecond laser pulses and noncollinear two-beam pump configuration.
4. To investigate the spatial, spectral and energy properties of the TH signal generated through noncollinear SWM and to optimize the spectral characteristics and generation efficiency of this TH of SWM radiation.
5. To demonstrate that measurements of the fifth-order intensity autocorrelations based on SWM of femtosecond laser pulses are suitable for the temporal characterization of such laser pulses.

## **NOVELTY AND PRACTICAL VALUE**

1. In contrast to other papers [1, 2] where reported spectral shifts of TH radiation were of the order of 3–4 nm and saturated quickly with the pump pulse energy, for the experiments we have used lenses of long focal lengths (1–2 m) which allowed us to increase the spectral shifts of TH signal to about 20 nm. Furthermore, the registered dependencies were not saturated and spectral shifts of TH radiation increased linearly with the pump pulse energy. Also note that TH spectral shifts were proportional to the measured plasma filament length which was also linearly dependent on the fundamental pulse energy.



2. The refocusing of femtosecond laser pulses which were forming the filament in air is studied both numerically and experimentally. It is shown that the refocusing of the pulse gives rise to enhanced spectral shifts of the fundamental and TH waves.
3. The efficiency of THG is limited due to the fact that its phase matching conditions can not be satisfied in a medium of normal dispersion, but we have demonstrated, that the a phase-matched frequency tripling of femtosecond laser pulses can be achieved by using noncollinear SWM through two-beam pump configuration. The energy measurements of TH pulse, generated through SWM, allowed us to estimate the magnitude of the quintic optical nonlinearity  $\chi_{xyyyx}^{(5)}(-3\omega, \omega, \omega, \omega, -\omega)$ .
4. We investigated the spectral and spatial properties of the THG by noncollinear SWM using two crossed laser beams with varying intensity ratio. This method allowed us to transfer the most of TH pulse energy into a single Gaussian output beam. Moreover, the spectral width of the TH signal generated via a SWM was at least by a factor of 2 narrower than that in the case of direct THG.
5. For the first time it was demonstrated that the fifth-order intensity autocorrelations based on SWM of femtosecond laser pulses can be used for the measurements of the laser pulse temporal duration and shape.

## **STATEMENTS TO DEFEND**

1. By focusing femtosecond laser pulses with lenses of long focal length ( $\sim 2$  m) in air the large spectral shifts of the pump and third harmonic waves (up to 20 nm and 50 nm, respectively) are taking place. These shifts depend linearly on the pump pulse energy and are proportional to the length of created light filaments also growing linearly with the pump pulse energy, which consequently increases the interaction length for the nonlinear effects that are inducing these spectral shifts (plasma generation, self-phase modulation and cross-phase modulation).
2. Refocusing of femtosecond laser pulses in air is taking place under the conditions of pulse focusing by the lenses of long focal length ( $\sim 2$  m), when the second filament is

formed and gives rise to the additional enhancement of the spectral blue-shift of the axial third harmonic due to the plasma electrons generated in the second filament. The refocusing does not change spectral red-shift of the third harmonic conical part because it is generated in the first filament and due to the off-axis propagation does not interact with the pump pulse and plasma electrons in the second filament.

3. By using six-wave mixing of femtosecond laser pulses in a medium of normal dispersion (air) the phase-matched third optical harmonic can be generated, when five pump photons are mixed together to create the third harmonic one. In the case of noncollinear pump beam configuration, when two pump beams are crossed at the phase-matching angle (13 mrad), the efficiency of this process can exceed  $10^{-4}$ .

4. The spatial and energy characteristics of third harmonic, generated via six-wave mixing in air can be optimized by varying the intensity ratio of the pump beams. This technique allows to transfer the most of generated third harmonic pulse energy into a single Gaussian beam, while the total generation efficiency can be increased up to 25 %, compared with the case of two equal intensity pump beams.

5. Six-wave mixing in air can be used for the temporal characterization of the femtosecond laser pulses, i.e., for the registration of the fifth-order intensity autocorrelations and FROG traces of these pulses. Due to the low air dispersion and small phase matching angles necessary for the six-wave mixing the extremely broad phase-matching bandwidths can be obtained (about 340), which support the measurements of pulse durations as short as 5 fs.

## **APPROBATION**

### **Scientific papers related to the topic of this thesis**

A1. V. Vaičaitis, V. Jarutis, **K. Steponkevičius**, and A. Stabinis, Noncollinear six-wave mixing of femtosecond laser pulses in air, *Phys. Rev. A* **87**, 063825 (2013).

A2. **K. Steponkevičius**, V. Pyragaitė, B. Makauskas, E. Žeimys, and V. Vaičaitis, Spectral shifts of the fundamental and third harmonic radiation in air induced by self-focused femtosecond laser pulses, *Opt. Commun.* **333**, 71-74 (2014).

A3. V. Pyragaitė, **K. Steponkevičius**, B. Makauskas, E. Žeimys, and V. Vaičaitis, Influence of refocusing of femtosecond laser pulses in air on third harmonic generation, *Opt. Commun.* **347**, 102-107 (2015).

A4. **K. Steponkevičius**, B. Makauskas, E. Žeimys, V. Jarutis, and V. Vaičaitis, Optimization of third harmonic generation in air by noncollinear six-wave mixing, *Laser Phys. Lett.* **12**, 063825 (2015).

A5. E. Gaižauskas, **K. Steponkevičius**, and V. Vaičaitis, Fifth-order intensity autocorrelations based on six-wave mixing of femtosecond laser pulses, *Phys. Rev. A* **93**, 023813 (2016).

### **Other scientific papers**

A6. V. Pyragaitė, V. Smilgevičius, **K. Steponkevičius**, B. Makauskas, and V. Vaičaitis, Phase shifts in terahertz wave generation by tightly focused bichromatic laser pulses, *J. Opt. Soc. Am. B* **7**, 1430-1435 (2014).

A7. D. Pentaris, D. Damianos, G. Papademetriou, A. Lyras, **K. Steponkevičius**, V. Vaičaitis, and T. Efthimiopoulos, Coherently controlled emissions  $|4P_{3/2,1/2}\rangle \leftrightarrow |4S_{1/2}\rangle$  from a femtosecond  $\Lambda$ -type excitation scheme in potassium atom, *J. Mod. Opt.* (2016).

### **Conference presentations (presented by Kęstutis Steponkevičius)**

1. **K. Steponkevičius**, V. Pyragaitė, V. Smilgevičius, and V. Vaičaitis, Nonlinear phase shifts of bichromatic pump waves during terahertz wave generation in air, CLEO/EUROPE - IQEC 2013, Munich, Germany (2013).

2. **K. Steponkevičius**, E. Žeimys, B. Makauskas, and V. Vaičaitis, Nonlinear interaction of femtosecond laser pulses and ambient air, 40<sup>th</sup> Lithuanian National Conference of Physics, Vilnius, Lithuania (2013).
3. **K. Steponkevičius**, V. Jarutis, B. Makauskas, E. Žeimys, and V. Vaičaitis, Phase-Matched Frequency Tripling of Femtosecond Laser Pulses in Air, Lasers and Optical Nonlinearity, Vilnius, Lithuania (2013).
4. **K. Steponkevičius**, V. Jarutis, and V. Vaičaitis, Noncollinear Third-Harmonic Generation of Femtosecond Laser Pulses in Air, Developments in Optics and Communications, Riga, Latvia (2014).
5. **K. Steponkevičius**, E. Gaižauskas, and V. Vaičaitis, Six-wave mixing in air for measurements of intensity autocorrelations of femtosecond laser pulses, 41st Lithuanian National Conference of Physics, Vilnius, Lithuania (2015).
6. **K. Steponkevičius**, and V. Vaičaitis, Fifth-order intensity autocorrelations of femtosecond laser pulses by noncollinear six-wave mixing, CLEO/EUROPE - IQEC 2015, Munich, Germany (2015).

**Conference presentations (Co-author of the presentation)**

1. **K. Steponkevičius**, V. Jarutis, and V. Vaičaitis, Quintic Optical Nonlinearity in Frequency Tripling of Femtosecond Laser Pulses, Photon14, London, England (2014).
2. V. Vaičaitis, V. Pyragaitė, **K. Steponkevičius**, and V. Smilgevičius, Broadband Terahertz Wave Generation From Air By Femtosecond Laser Pulses, 15th International Symposium on “Ultrafast Phenomena in Semiconductors” (15-UFPS), Vilnius, Lithuania (2013).
3. V. Pyragaitė, V. Smilgevičius, **K. Steponkevičius**, B. Makauskas, and V. Vaičaitis, Phase Shifts of Bichromatic Pump Pulses in Terahertz Wave Generation from Laser Induced Gas Plasma, Lasers and Optical Nonlinearity, Vilnius, Lithuania (2013).
4. V. Pyragaitė, **K. Steponkevičius**, V. Smilgevičius, and V. Vaičaitis, Broadband Terahertz Wave Generation from Laser-Induced Air Plasma, Photon14, London, England (2014).

5. V. Pyragaitė, **K. Steponkevičius**, B. Makauskas, E. Žeimys, and V. Vaičaitis, Third harmonic generation in air induced by laser pulses: refocusing and spectral shifts, 41st Lithuanian National Conference of Physics, Vilnius, Lithuania (2015).

## CO-AUTHORS CONTRIBUTION

K. Steponkevičius performed all the experiments described in this thesis in Vilnius University, Laser Research Center during the period 2012–2016. Also author performed part of the numerical analysis and comparison of the theoretical results with the experimental data (in A2, A4 and A5 publications). However, it is very important to mention the contribution of these co-authors:

1. Dr. **V. Vaičaitis** (A1–A5) supervised the research of noncolinear six-wave mixing and third harmonic generation in air. Also V. Vaičaitis helped to interpret the results and present them to scientific community.
2. Prof. **A. Stabinis** (A1) has performed theoretical analysis of the noncolinear six-wave mixing in air and helped to publish the paper.
3. Dr. **V. Jarutis** (A1, A4) developed a theoretical model of noncolinear six-wave mixing, helped to interpret and publish the papers.
4. Dr. **V. Tamulienė (Pyragaitė)** (A2, A3) theoretically analysed and interpreted the results of third harmonic generation and refocusing in air and helped to publish the papers.
5. Dr. **E. Gaižauskas** (A5) performed theoretical calculations of the fifth-order intensity autocorrelations based on six-wave mixing of femtosecond laser pulses and helped to publish the paper.
6. Students **B. Makauskas** and **E. Žeimys** (A2–A4) helped to perform the experiments of third harmonic generation and noncolinear six-wave mixing.

# 1. THIRD HARMONIC GENERATION IN AIR

## 1.1. EXPERIMENTAL METHODS

In our experiments TH was generated in atmospheric air by focused femtosecond laser pulses. All experiments were performed using a Ti:sapphire laser system, which generated the ultrashort light pulses of 35 fs, 100 fs or 120 fs (FWHM) duration  $\tau$  with a central wavelength of 800 nm at a repetition rate of 1 kHz, single pulse energy of up to 3 mJ (Fig. 1.1.1). The diameter of the Gaussian laser beam at the  $1/e^2$  level was about 8 mm. Laser pulse energy could be varied by a half-wave plate and two polarizers. The pump beam was focused using lenses of various focal lengths.

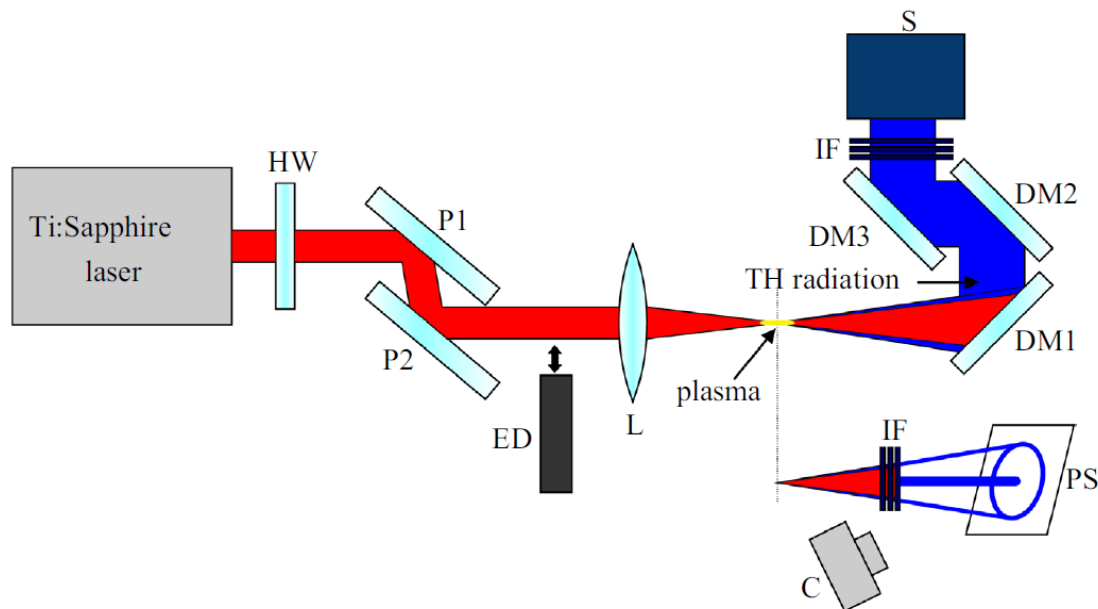


Fig. 1.1.1. Schematic of the experimental setup: HW, half-waveplate; P1–P2, polarizers; ED, energy detector; L, focusing lens; DM1–DM3, dichroic mirrors; IF, interference filters; S, spectrometer; C, digital camera; PS, paperscreen.

The TH was generated in a plasma filament created in air by the fundamental harmonic (FH) laser pulses. From the fundamental radiation the TH signal was separated using the dichroic mirrors and interference filters. Spectral characteristics of TH were registered using a spectrometer. During these measurements the conical and central parts of TH signal were focused into the fiber delivering light to the spectrometer. In addition to these measurements, the fluorescence images produced on the paper screen of the far-

field TH radiation were registered by digital camera. In all experiments the pulse energy of the pump beam was controlled by using the energy detector.

## 1.2. SPATIAL, SPECTRAL AND ENERGY CHARACTERISTICS OF THIRD HARMONIC GENERATION

In the case of high laser pulse energies (more than 1mJ per pulse) a bright blue TH central spot surrounded by the ring has been observed on the screen. Typical experimentally registered far-field patterns of the TH emission are shown in Fig. 1.2.1. Note that the divergence of TH conical part have not depended on the FH pulse energy  $E$ , but decreased with the focusing lens focal length  $f$ . When the lenses of short focal length ( $f \leq 300$  mm) were used, the conical and central parts of TH overlapped in space and the spatial structure of the far-field radiation was not distinct (Fig. 1.2.1. (a)).

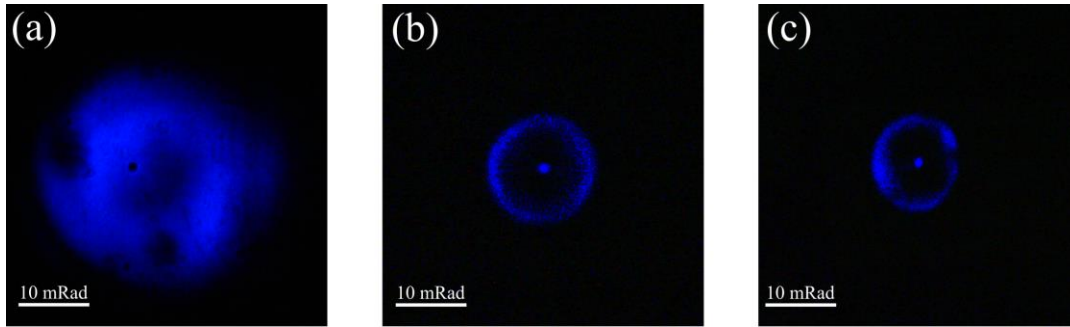


Fig. 1.2.1. Experimentally registered far-field patterns of TH beam observed using (a) 300 mm, (b) 1000 mm, and (c) 1400 mm focal length focusing lenses. Laser pulse duration  $\tau = 120$  fs.

In order to estimate the interaction length of the FW and TH pulses, we have measured the dependencies of the plasma filament length  $L$  on the FH pulse energy  $E$  for different focal lengths of focusing lenses (Fig. 1.2.2.). Thus, when the visible by naked eye plasma column appeared, the registered by a CCD camera filament length was found to be about 5 cm (note that in this case the Rayleigh length  $z_R = \pi w_0^2 / \lambda \approx 6.3$  cm, where  $\lambda = 800$  nm is the wavelength,  $w_0 = 127$   $\mu$ m is the beam waist for  $f = 1$  m).

In the case of higher pump pulse energies the plasma column length linearly increased with  $E$  (see Fig. 1.2.2. (b)). The slope values of linear fit were the following:

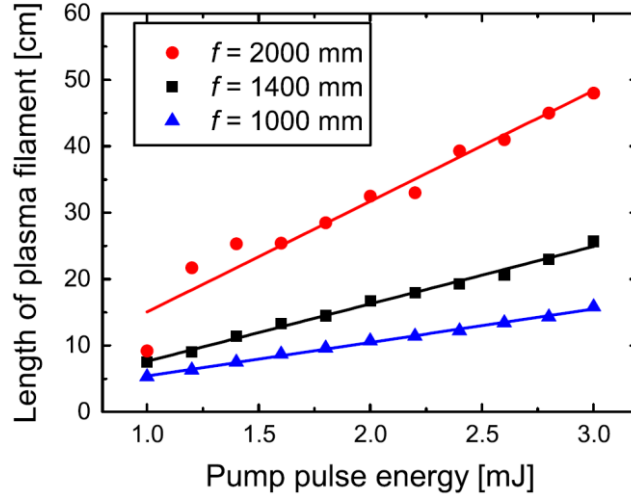


Fig. 1.2.2. Dependencies of the plasma filament length  $L(E)$  on the FH pulse energy  $E$  for the lenses of different focal lengths  $f$  (the dots are the experimental data and the lines present the linear fits). Laser pulse duration  $\tau = 120$  fs.

15.9 cm/mJ ( $f = 2000$  mm), 8.2 cm/mJ ( $f = 1400$  mm) and 5.2 cm/mJ ( $f = 1000$  mm). Note that the length of the plasma column increased faster for the lenses of longer focal length  $f$ . Note also that for  $E = 1$  mJ, the peak power  $P_0 = E / \tau = 7.8$  GW (for the Gaussian pulse of 120 fs duration at FWHM) is larger than the critical power  $P_{cr} = 2.9$  GW, which is estimated using the expression:

$$P_{cr} = \frac{\lambda^2}{8n_0n_2} \quad (1.2.1)$$

where  $n_0$  and  $n_2 = 3,2 \times 10^{-19}$  W/cm<sup>2</sup> are the linear and nonlinear refractive indexes of air, respectively). Note that the self-focusing and plasma filaments appeared for all the used focal length lenses. Thus, the plasma formation onset was strongly dependent on  $P$  but weakly depended on  $f$  under our experimental conditions. Note that the THG conversion efficiency was of the order of  $10^{-6} - 10^{-5}$  for  $E = 2$  mJ and lenses of focal lengths of  $f = 1000-2000$  mm.

The FH spectral broadening registered beyond the filament is illustrated in Fig. 1.2.3. (a). The spectra of FH were registered using long focal length ( $f = 2000$  mm) lens because it forms the long plasma filament (up to 50 cm) (see Fig. 1.2.3. (b)) and as a result the spectral broadening is larger than that obtained using lenses of shorter focal length. As one can see (see Fig. 1.2.3. (a)), the FH spectra consist of the blue-shifted and red-shifted parts with respect to the central pump wavelength of 800 nm, when  $E > 1$  mJ.



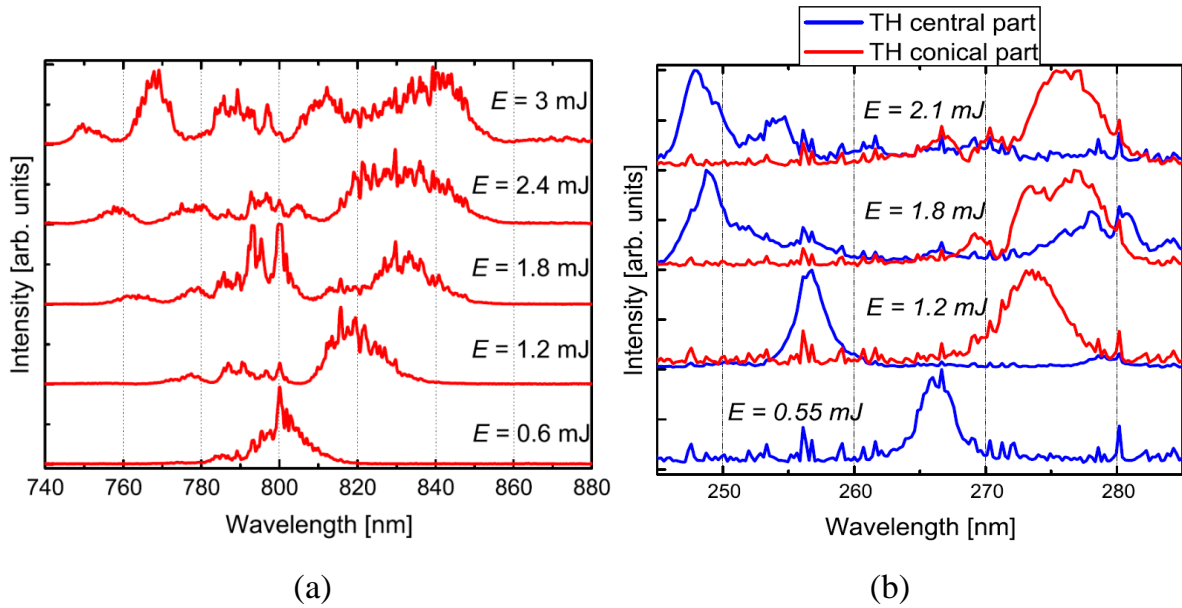


Fig. 1.2.3. Experimentally registered (a) FH and (b) TH spectra at different pump pulse energies  $E$  using the lens of focal length  $f = 2000$  mm. Laser pulse duration  $\tau = 120$  fs.

In addition, the peak wavelength of TH conical part (of about 274 nm) was linearly dependent on the FH pulse energy  $E$  and red-shifted with respect to the central pump wavelength divided by three (see Fig. 1.2.3. (b)). However, when  $E$  was less than 0.55 mJ, the peak wavelength of TH central part was about 266 nm, which corresponds to the non-shifted TH wavelength. In contrast to the conical TH emission, the spectra of TH central part were blue-shifted with respect to the wavelength of 266 nm and strongly depended on  $E$  (Fig. 1.2.4.).

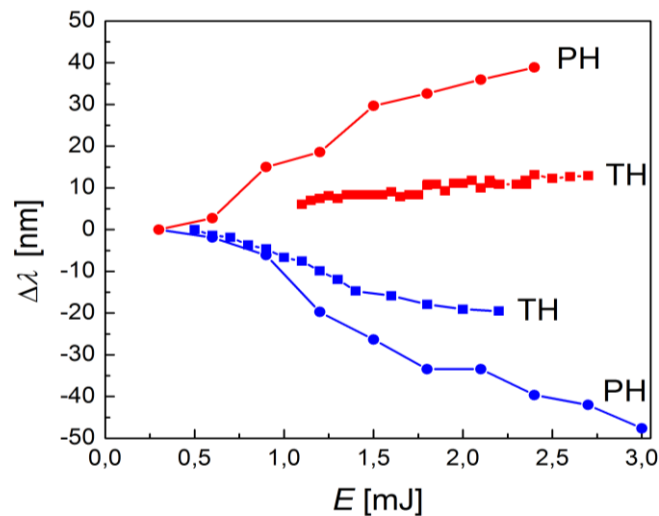


Fig. 1.2.4. Experimentally registered dependencies of the blue- and red- shifts of the FH (circles) and TH (rectangles) on the pump pulse energy  $E$  for  $f = 2000$ mm and  $\tau = 120$  fs.

### 1.3. SPECTRAL SHIFTS OF THIRD HARMONIC RADIATION AND REFOCUSING OF FEMTOSECOND LASER PULSES

The explanation of filamentation of femtosecond laser pulses is based on self-focusing due to the nonlinear Kerr effect and multiphoton ionization which stops the growth of laser beam intensity [27]. Then the intensity clamping takes place [42, 43]. The losses due to the ionization process may be low so that later, when the defocusing starts, the self-focusing due to nonlinear Kerr effect may be repeated. This process is called refocusing [51, 52]. This motivated us to investigate the influence of refocusing to the enhanced spectral shifts of the fundamental and TH.

Therefore, we simulated numerically the equation for the plasma electron density and nonlinear coupling equations for the FH and TH waves which can be found in Ref. [A3] (introduction chapter). First, we demonstrate that multiple refocusing can be obtained at a moderate FH pulse energy of 2.2 mJ (Fig. 1.3.1.). Indeed, our experiment showed the refocusing which was confirmed by the numerical simulations. As we can see from Fig. 1.3.2, the main part (with the largest electron density) of the filament is created before the lens focus at  $z = 2$  m.



Fig. 1.3.1. Experimentally registered filaments. Energy 1.5 mJ (a) and 2.2mJ (b), pulse duration 35 fs,  $f = 2000$  mm. (b) picture illustrates the refocusing of the FH beam.

After passing the focus, the beam power is sufficient for refocusing, therefore the additional filaments appear. Depending on initial pump pulse energy, the refocusing takes place once ( $E = 1.5$  mJ, black solid curve in Fig. 1.3.2.) or twice ( $E = 2.2$  mJ, red dashed curve). We note that the refocusing was already described and experimentally demonstrated in previous reports [4–6]. However, we performed the experiment using the lens with long focal length. In addition, the laser beam parameters were close to the

parameters of the experiment described in 1.2. chapter, when large spectral shifts of the FH and TH were observed.

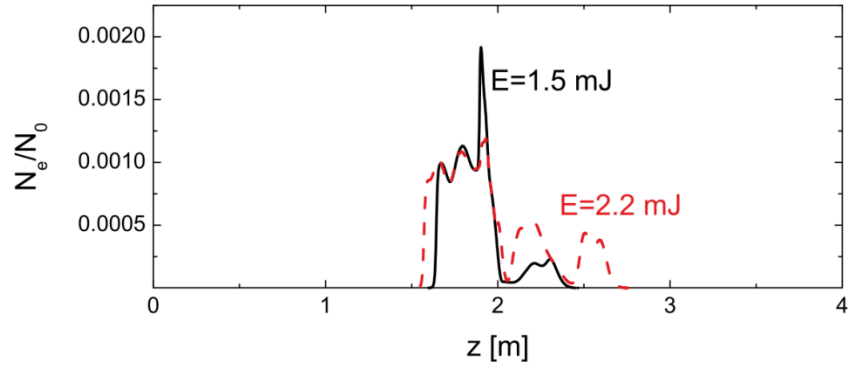


Fig. 1.3.2. Dependence of plasma density on the distance from the lens  $z$ . Energy 1.5mJ (black solid line) and 2.2mJ (dashed line), pulse duration 35 fs,  $f = 2000$  mm.

In Fig. 1.3.2., we show the numerically calculated plasma density in the filament created by the 100 fs long pulse with an energy of 1.5mJ. Comparison of Figs. 1.3.2. and 1.3.3. shows that both pulse durations (35 fs and 100 fs) can give rise to the refocusing. We note that the filament formed by the pulse with an energy of 1.5 mJ is longer for the longer input pulse.

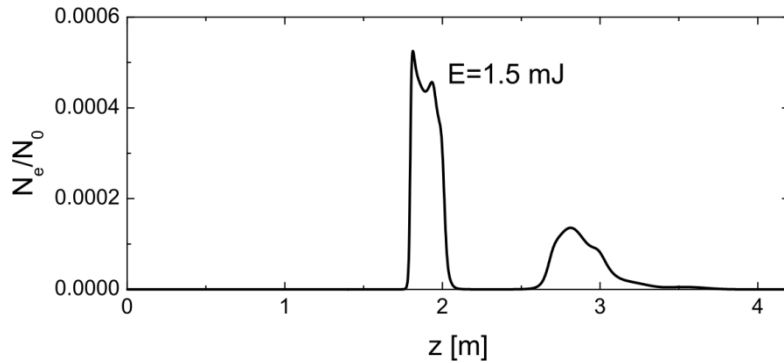


Fig. 1.3.3. Dependence of plasma density on the distance from the lens  $z$ . FH pulse energy 1.5mJ, pulse duration 100 fs and  $f = 2000$  mm.

At a duration of 100 fs (Figs. 1.3.3), the filament is more than 1 m long, the most powerful part is created before the focus and the refocusing takes place afterwards. In Figs. 1.3.4 and 1.3.5, we show the dynamics of the FW and TH pulsed beams during the propagation in air. We note that the pulse evolution before the beam refocusing ( $z < 2.5$  m) is similar to the one described in Ref. [1, 2]. Thus, the conical part of TH is present

and the cone angle is  $\sim 10$  mrad. The conical TH part is not visible in Fig. 1.3.5, however it was found by the numerical calculation of the first maximum position of TH. At  $z = 2.0$  m the FW pulse splits into two pulses. At  $z = 2.5$  m refocusing starts, and again we see the formation of single pulse. At this point, the beam is refocused. Afterwards, the pulse splits again ( $z = 3.5$  m). One may notice, that the TH pulse dynamics closely follows the evolution of the FW pulse.

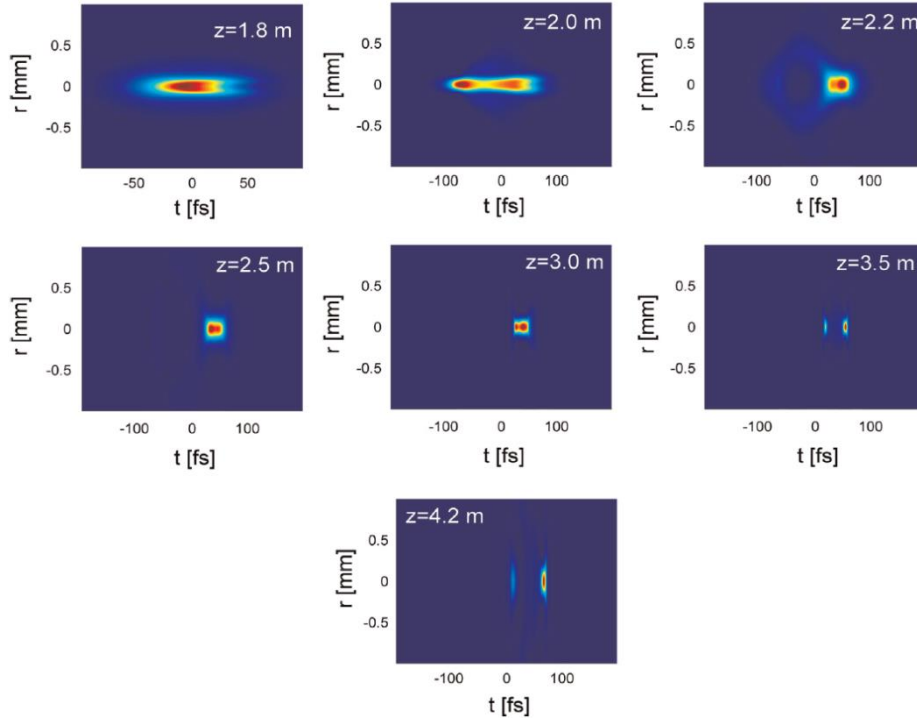


Fig. 1.3.4. Spatio-temporal profiles of FH pulse at different distances from the lens  $z$ . FH pulse energy 1.5 mJ, pulse duration 100 fs and  $f = 2000$  mm.

In Figs. 1.3.6 and 1.3.7, we show the evolution of the FH and TH spectra. TH spectra are shown for the central and conical parts. The FH spectrum was integrated over the radial coordinate. As we can see from Fig. 1.3.6 the blue- and red-shifts appear in TH central and conical parts, respectively. The blue-shift is moderate, of several nm (6 nm) and the red-shift is 38 nm at  $z = 2.5$  m. Further, the refocusing starts and the central TH part is shifted to the red side. The red-shift is 5 nm at  $z = 3$  m and turns to the blue-shift at  $z = 3.5$  m, see Fig. 1.3.7. The spectrum of the conical part does not change considerably because it mainly consists of the radiation which was generated before the refocusing. Finally, at  $z = 4.2$  m, the plasma density decreases and a large TH blue-shift of more than 10 nm (28 nm) is obtained. The red-shift of the TH conical part is 37 nm.

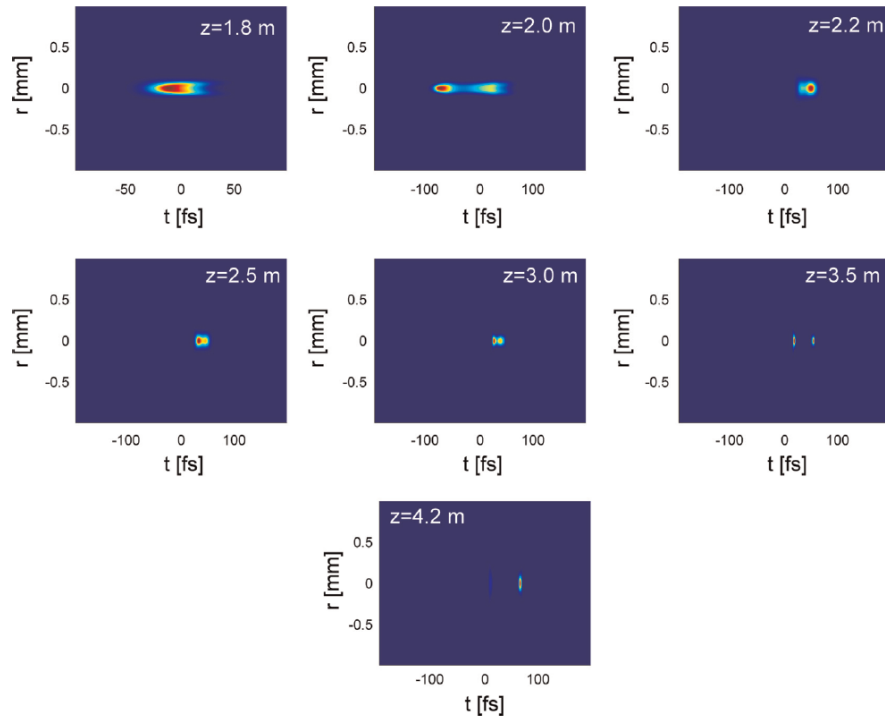


Fig. 1.3.5. Spatio-temporal profiles of TH pulse at different distances from the lens  $z$ . FH pulse energy 1.5 mJ, pulse duration 100 fs and  $f = 2000$  mm.

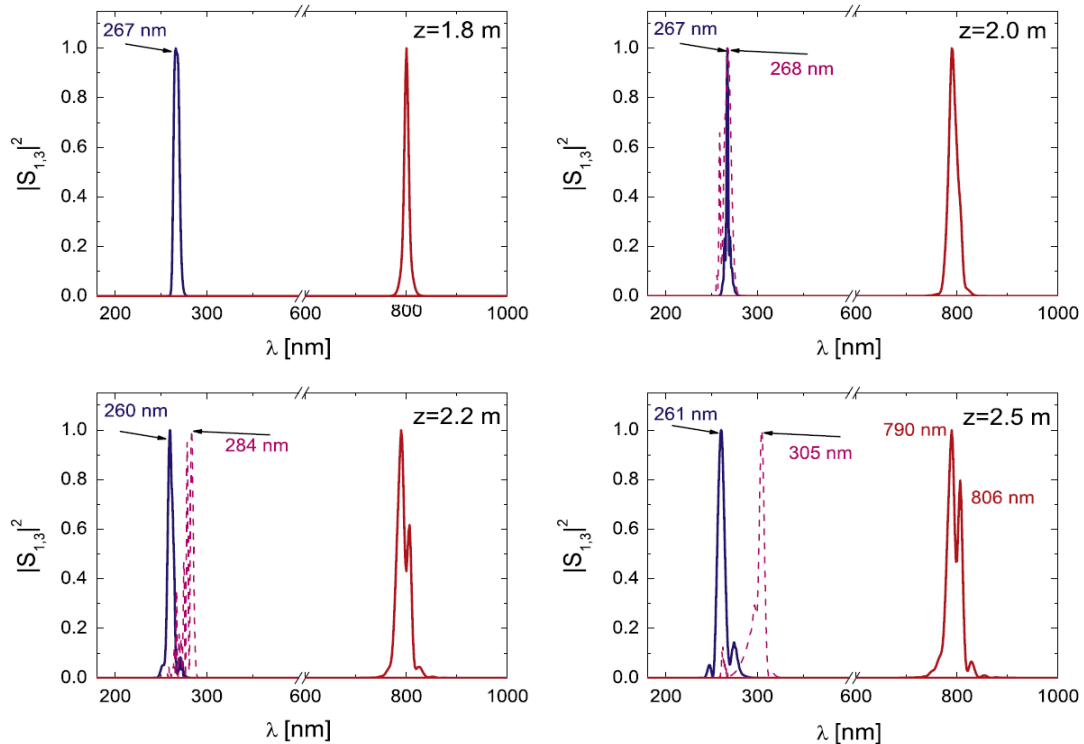


Fig. 1.3.6. Spectra of the integrated fundamental wave (solid red line), axial TH wave (solid blue) and conical TH wave (dashed magenta). Different distances from the lens,  $z$  [m]: 1.8; 2.0; 2.2; 2.5. FH pulse energy 1.5mJ, pulse duration 100 fs and  $f = 2000$  mm. The spectral shifts are small before the refocusing.

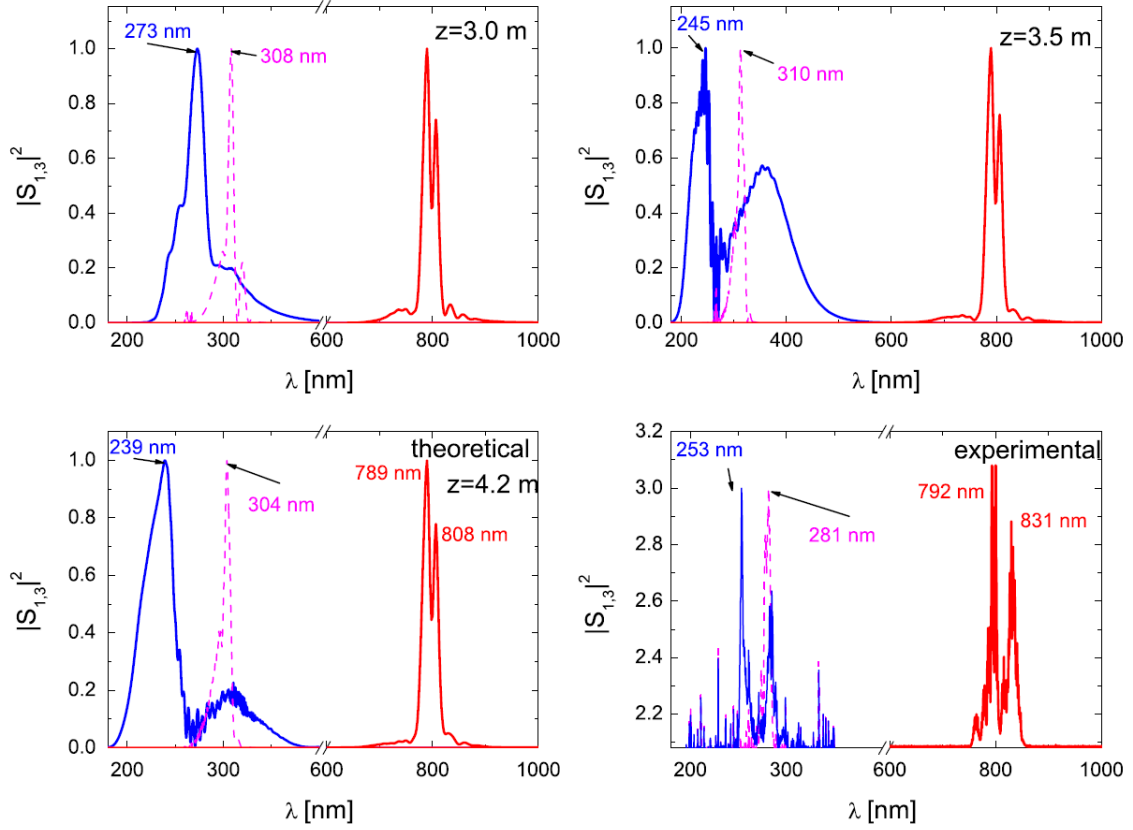


Fig. 1.3.7. Spectra of the integrated fundamental wave (solid red lines), axial TH wave (solid blue lines) and conical TH wave (dashed magenta). Different distances from the lens,  $z$  [m]: 3.0; 3.5; 4.2. FH pulse energy 1.5 mJ, pulse duration 100 fs and  $f = 2000$  mm. The spectral shifts become larger after the refocusing. The last graph depicts the spectra recorded by the spectrometer at the FH pulse energy of 1.8mJ, pulse duration 100 fs and  $f = 2000$  mm.

Note that the large spectral shifts of TH can be seen in the last graph of Fig. 1.3.7, where the experimental spectra are depicted (blue-shift of 14 nm and red shift of 14 nm). We also note a red-shifted component in the central part of TH beam (blue curves), which can be seen both in numerical (at  $z = 4.2$  m) and experimental data. Note that the refocusing enhances not only the blue-shift of the central part of the TH beam. The blue- and red-shifts of the FH also increase, compare the values at  $z = 2.2$  m in Fig. 1.3.6 (blue-shift of 10 nm and red-shift of 6 nm) and at  $z = 4.2$  m in Fig. 1.3.7 (11 nm and 8 nm, respectively).

In conclusion, we have studied the refocusing process as well as pulse evolution of FH and TH pulses inside the filament. The presented results elucidate the connection

between the refocusing and large spectral shifts which were experimentally observed and described in chapter 1.2. The refocusing gives rise to enhanced spectral blue-shift of the central part of TH wave. Enhanced blue- and red- shifts are also obtained for the FH. The conical part of the TH beam is formed in the first focusing cycle, so its spectral red-shift does not change considerably during the propagation in the filament.

## **2. NONCOLLINEAR SIX-WAVE MIXING IN AIR**

### **2.1. EXPERIMENTAL METHODS**

For the experiments of noncollinear six-wave mixing in air we have used a 1 kHz repetition rate femtosecond Ti:sapphire laser system delivering 35fs, 100 fs or 130 fs (FWHM) light pulses centered at 800 nm with a pulse energy of 3 mJ (Fig. 2.1.1). The diameter of the Gaussian beam at the  $1/e^2$  level was about 8 mm. The laser pulse energy could be varied by an attenuator composed of a zero-order half-wave plate and a broadband polarizer. Then the fundamental laser beam was divided into two orthogonally polarized pump beams by the additional polarizer and half-wave plate, which also allowed us to adjust the beam intensity ratio by transferring the pulse energy from the one beam to another. The polarization state of the beams was controlled by the additional half-wave plate inserted into the path of one of the beams. However, since light waves of the linear orthogonal polarizations do not interfere and, thus, do not create the spatial intensity modulations which result in more efficient ionization of air molecules, all our experiments of six-wave mixing were performed with orthogonally polarized pump beams. Both laser beams were focused in air by a 100 cm focal length lens, creating two 5–10 cm long filaments for the pump pulse energies of more than 0.5 mJ. Each filament produced a weak TH signal consisting of a central spot surrounded by a ring [1, 2]. However, when the laser beams were crossed at a small angle in the focal plane of the lens and the pump pulses were overlapped in time, the two bright TH beams outside the crossed pump were observed. Therefore, the TH and fundamental laser beams were well separated spatially. However, in order to increase the signal / noise ratio for the TH energy measurements we have also used the additional dichroic mirrors

and calibrated optical filters. Note that though the two TH beams could be observed for a wide range of the pump beam crossing angle, the most efficient THG was observed at the angle of about 10-13 mrad.

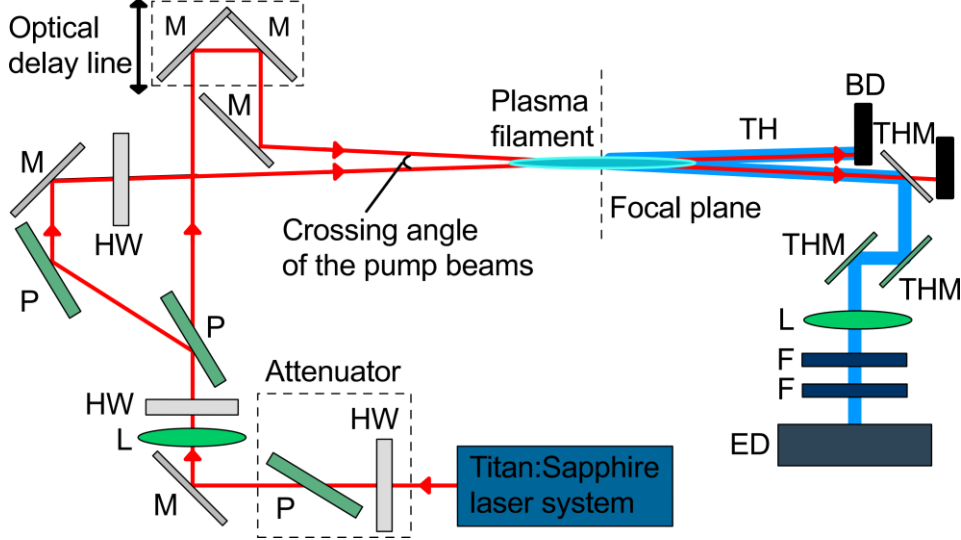


Fig. 2.1.1. Schematic of the experimental setup: HW, half-wave plate; P, polarizer; M, dielectric mirror; L, focusing lens; BD, beam dump; THM, TH mirror; F, optical filter; ED, energy detector.

## 2.2. SPATIAL, SPECTRAL AND ENERGY CHARACTERISTICS OF NONCOLLINEAR SIX-WAVE MIXING

For the theoretical treatment of SWM we assume that the pump pulses propagate in slightly different directions along the wave vectors  $\vec{k}_1$  and  $\vec{k}'_1$ . The noncollinear THG in air can be described via the fifth order susceptibility tensor  $\chi_{q,p_1,p_2,p_3,p_4,p_5}^{(5)}(-3\omega; \omega, \omega, \omega, \omega, -\omega)$ , where the indices  $q$  and  $p_j (j = 1, \dots, 5)$  denote the polarization of the TH and pump waves, respectively. The wavevector diagram illustrating phase-matched frequency tripling in isotropic normally dispersive media is sketched in Fig. 2.2.1 (b). One can see that in this case the TH wave vectors are directed outward with respect to the intersecting crossed laser beams. Note that in the plane-wave approximation:

$$n_1 \cos \alpha = n_3 \cos \beta, \quad (2.2.1)$$

$$5n_1 \sin \alpha = 3n_3 \sin \beta. \quad (2.2.2)$$



So the phase matching occurs when the pump beams intersect at an angle  $2\alpha_0 \approx \sqrt{9\Delta n/2} \approx 10$  mrad, where  $\Delta n = n_3 - n_1$ , and  $n_1$  and  $n_3$  are the refractive indices of air for the FH and TH waves, respectively. In addition, based on the symmetry properties of the  $\chi^{(5)}$  tensor one can deduce that in our experimental configuration THG via SWM is possible only through the fifth-order susceptibility tensor component  $\chi_{xxxxxx}^{(5)} = \chi_{yyyyyy}^{(5)}$  for the both pump beams of the same polarization and through the component  $\chi_{xyyyyx}^{(5)} = \chi_{yxxxxx}^{(5)}$  for the orthogonally polarized laser beams. In the former case the polarizations of all interacting waves are the same, while in the latter, the polarizations of each TH beam should be orthogonal to that of the adjacent pump beam.

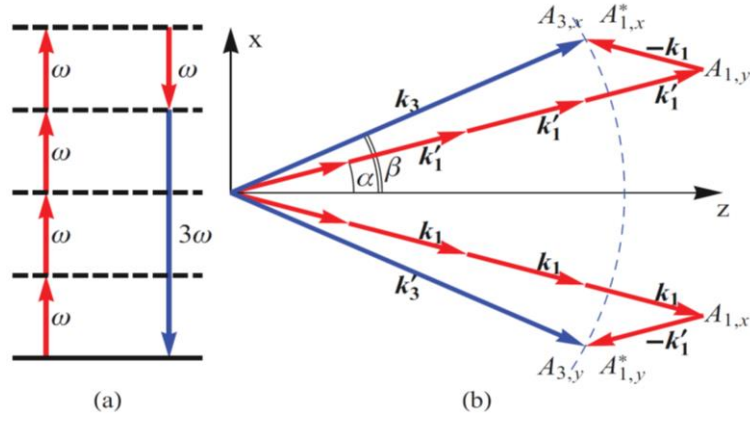


Fig. 2.2.1. (a) Photon energy diagram and (b) wavevector diagram of noncollinear SWM.

Our noncollinear six-wave-mixing model is described under the nondepleted pump approximation by a set of equations which can be found in Ref. [A1] (introduction chapter). When the FH pulses overlapped in space and time, as predicted by the theory (see Fig. 2.2.1. (b)), two bright TH beams outside the crossed pump were observed on a screen for a wide range of beam crossing angles. Typical experimentally registered far-field patterns and polarizations of the pump and TH produced by the SWM interaction are shown in Fig. 2.2.1. (c). As can be seen, the TH signal consists of two orthogonally polarized spots at the locations well predicted theoretically. An even better match between the experimental data and theory can be seen in the dependence of the normalized energy of the TH generated noncollinearly on the crossing angle  $2\alpha$  of the pump beams (Fig. 2.2.3). From this correspondence, taking the absolute values of the TH pulse energy, we have estimated the value of  $\chi_{xyyyyx}^{(5)}(-3\omega; \omega, \omega, \omega, \omega, -\omega) \approx 2 \times 10^{-49}$

$(\text{m/V})^4$ . Note that the TH signal could be easily registered for low laser pulse energies (of less than 200  $\mu\text{J}$  for each pump beam), when no apparent filamentation and laser-induced plasma formation evidence could be observed, which indicates that plasma-related effects play little role in our experiment. The experimentally registered dependencies of the TH signal on the pump-pulse energy also showed a good agreement with theoretical predictions. Thus, as can be shown from Eqs. (1) and (2) in Ref. [A1], while the total TH yield should be proportional to the fifth power of the pump intensity (Fig. 2.2.4.), the power of each TH beam should scale as the product of  $I_{1,x}I_{1,y}^4$  and  $I_{1,y}I_{1,x}^4$ , where  $I_{1,p}$  corresponds to the intensity of the pump beam. This has been confirmed experimentally (see Fig. 2.2.5. (a) and 2.2.5. (b)) over the full range of available laser powers and additionally indicates that during such SWM each TH photon results from the combination of four photons from one laser beam and a single photon from the other.

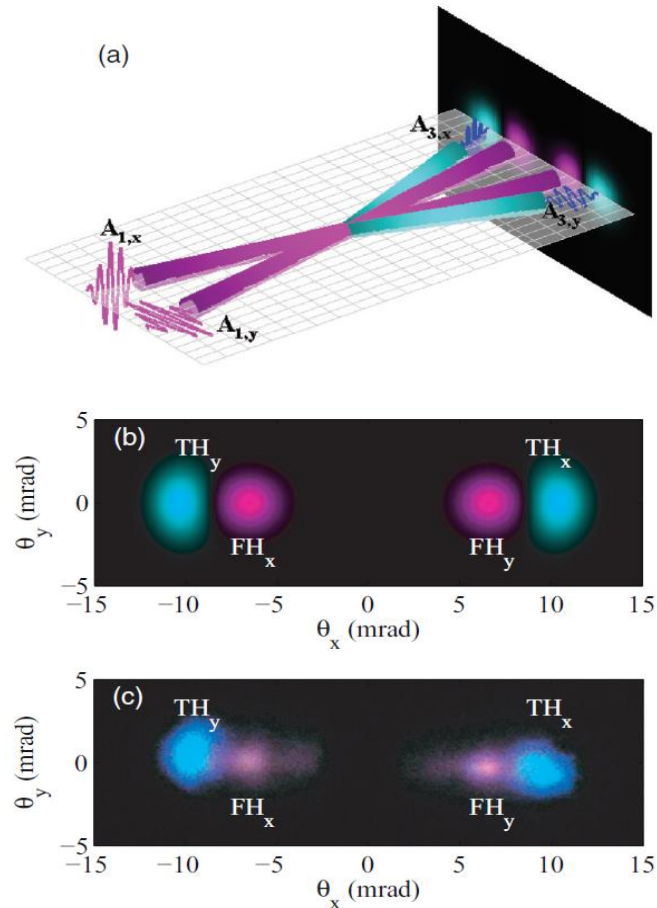


Fig. 2.2.1. (a) Experimental configuration illustrating a two-beam SWM in air with the far-field patterns of the fundamental and TH for a beam crossing angle of 13 mrad (the total energy of both laser pulses was about 1.9 mJ, pulse duration 100 fs); (b) numerical simulations; and (c) the experimentally obtained data.

At the maximum laser-pulse energy of about 2 mJ the total TH output could reach over 200 nJ, which corresponds to a conversion efficiency of about  $10^{-4}$ . Note, however, that the maximum TH pulse energy generated by a single laser beam, focused by a lens of the same focal length, did not exceeded a few nanojoules; thus, under the given experimental conditions, the noncollinear THG was about by two orders of magnitude more efficient.

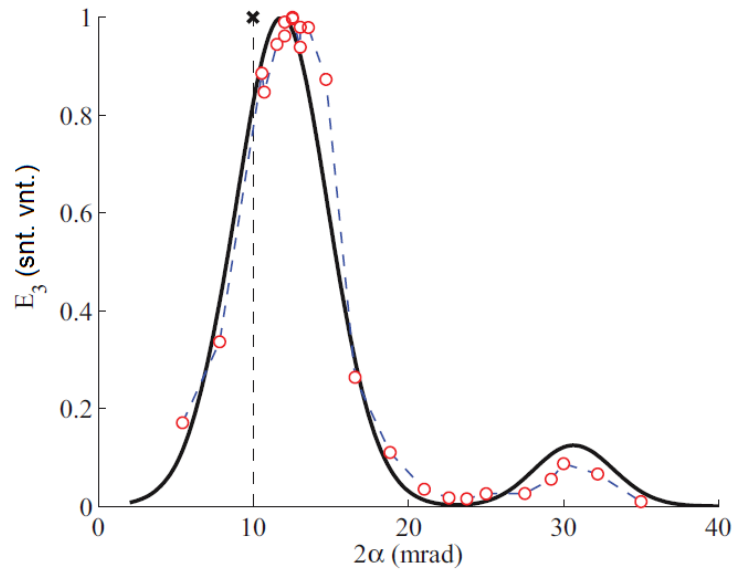


Fig. 2.2.3. Dependence of TH yield  $E_3$  of noncollinear SWM on the beam crossing angle  $2\alpha$  (pulse duration 100 fs). The vertical dashed line corresponds to the plane-wave approximation.

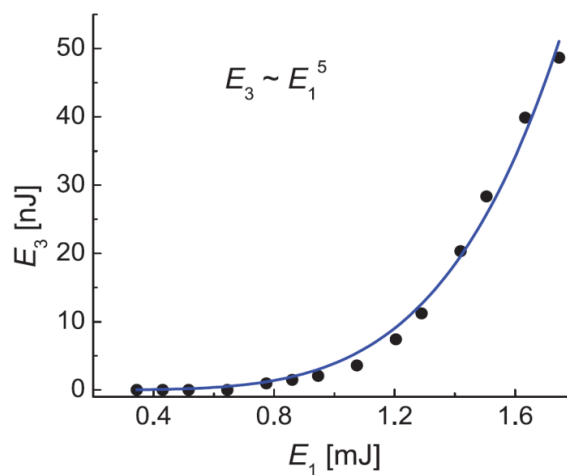


Fig. 2.2.4. Dependence of the total TH pulse energy  $E_3$  on the total pump pulse energy  $E_1$  for the pump beam intensity ratio of 1 : 1 and pulse duration 100 fs (the dots are the experimental data and the line presents the theoretical fifth power fit).

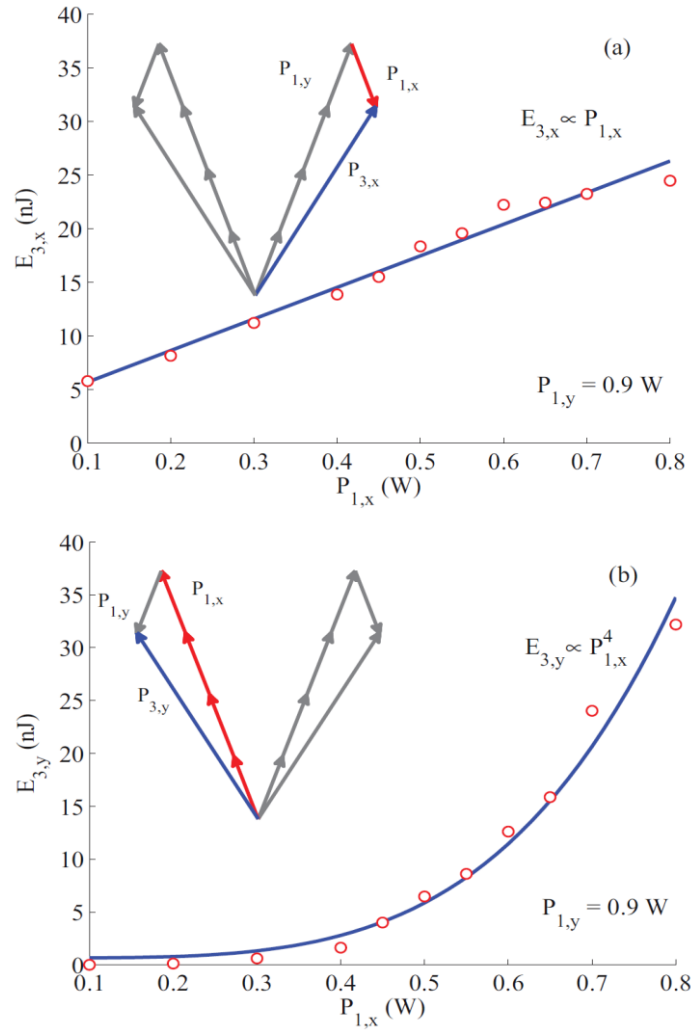


Fig. 2.2.5. Dependence of the single-beam TH yield of SWM on a single laser-beam power for (a) constant and (b) varying adjacent laser beam energies.

By varying the pump beam intensity ratio we have demonstrated a possibility to transfer the TH fluence into a single beam. Thus, at the pump beam intensity ratio of 1 : 1 the energy of the TH signal was confined in the two equal intensity output beams, while for the significantly different pump beam intensity ratios most of the TH output was concentrated into a single TH beam, which corresponds well to the SWM model (see Fig. 2.2.6. (a) and (b)).

To explain the energy transfer phenomenon we assume that the total pump beam pulse energy  $E_1 = E_{1,x} + E_{1,y}$ , where  $E_{1,x}$  and  $E_{1,y}$  are the pulse energies of the separate pump beams as shown in a wave vector diagram of Fig. 2.2.7. (a), where indexes 1 and 3 denote the fundamental and TH waves, respectively, and  $x$  or  $y$  indexes indicate the wave polarization along the  $x$  or  $y$  axis. Similarly, the total TH pulse energy can be written as

$E_3 = E_{3,x} + E_{3,y}$ , where  $E_{3,x}$  and  $E_{3,y}$  are the pulse energies of each TH beam, which can be written in the form:

$$E_{3,x} \propto E_{1,x}E_{1,y}^4 = (E_1 - E_{1,y})E_{1,y}^4, \quad (2.2.3)$$

$$E_{3,y} \propto E_{1,y}E_{1,x}^4 = E_{1,y}(E_1 - E_{1,y})^4. \quad (2.2.4)$$

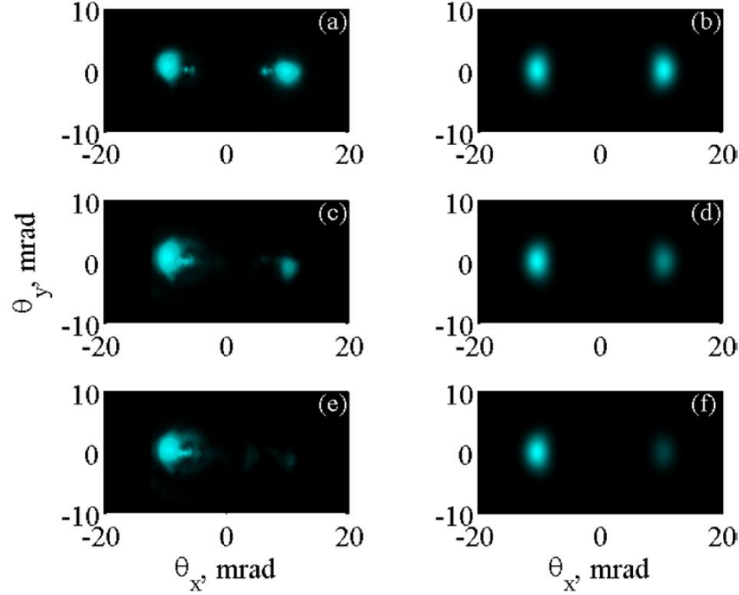


Fig. 2.2.6. Experimentally registered (a), (c), (e) and numerically simulated (b), (d), (f) far-field TH patterns for  $E_1 = 2$  mJ and the beam intensity ratio of 1 : 1 (a), (b), 1 : 2 (c), (d) and 1 : 3 (e), (f). FH pulse duration 100 fs.

From Eqs. (2.2.3) and (2.2.4) one can easily find that the concentration of the pump energy into a single beam consequently leads to the generation of one strong and one weak TH beam. The dependencies of TH pulse energies on the pump beam intensity ratio, calculated using equations (2.2.3) and (2.2.4) were compared with the experimentally obtained values (see Fig. 2.2.7). A reasonably good agreement can be seen in the dependencies of TH pulse energy in each separate TH beams (Fig. 2.2.7. (a)) and in total TH yield (Fig. 2.2.7. (b)) on single pump beam pulse energy  $E_{1,y}$ .

Note that the derivatives of equations (2.2.3) and (2.2.4) are equal to zero and consequently the single beam TH energy is maximal, when the normalized pump pulse energy  $E_{1,y}$  values are 0.2 and 0.8. This corresponds to the pump beam intensity ratio  $E_{1,y} / E_{1,x}$  of 1 : 4 and 4 : 1, respectively (see Fig. 2.2.7. (a)). In addition, as predicted by equations (2.2.3) and (2.2.4) at these points (for  $E_{1,y}$  values of 0.2 and 0.8) we obtained a

significant increase (about 25%) of TH pulse energy compared with the case of the pump beam intensity ratio of 1 : 1 (see Fig. 2.2.7. (b)).

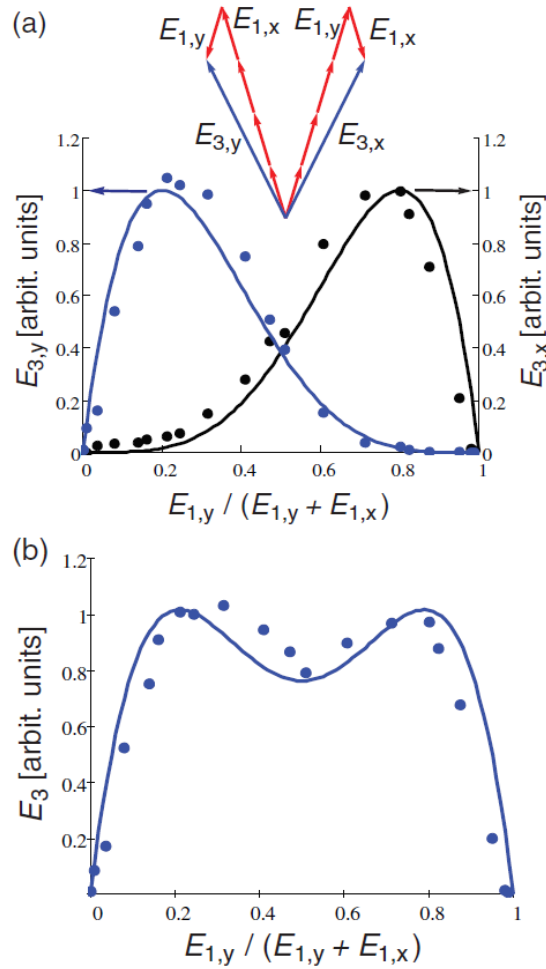


Fig. 2.2.7. (a) Dependencies of (a) separate TH beam pulse energies ( $E_{3,y}$  and  $E_{3,x}$ ) and (b) total TH pulse energy  $E_3$  on single pump beam pulse energy  $E_{1,y}$  for  $E_1 = 2$  mJ and pulse duration 100 fs (the dots are the experimental data and the lines present the theoretical fits).

During the experiment we have also investigated the spectral properties of TH radiation generated through noncollinear SWM (see Fig. 2.2.8. (a)). Thus, when  $E_1$  was less than 1 mJ, the TH peak wavelength was about 267 nm, which corresponds well to the central wavelength of the fundamental wave. However, the TH spectra were slightly red-shifted at higher pump powers (for example, approximately by 1.6 nm at  $E_1 = 2$  mJ). In addition, the spectral width of the TH radiation was only about 3 nm (FWHM) and we did not observe its broadening with pump power. This is in sharp contrast with

the case of single beam pump configuration, when the complicated spatial and spectral properties of the TH signal usually are observed even at the low pump power levels (see Fig. 2.2.8. (a), chapter 1.2. and [1, 2]).

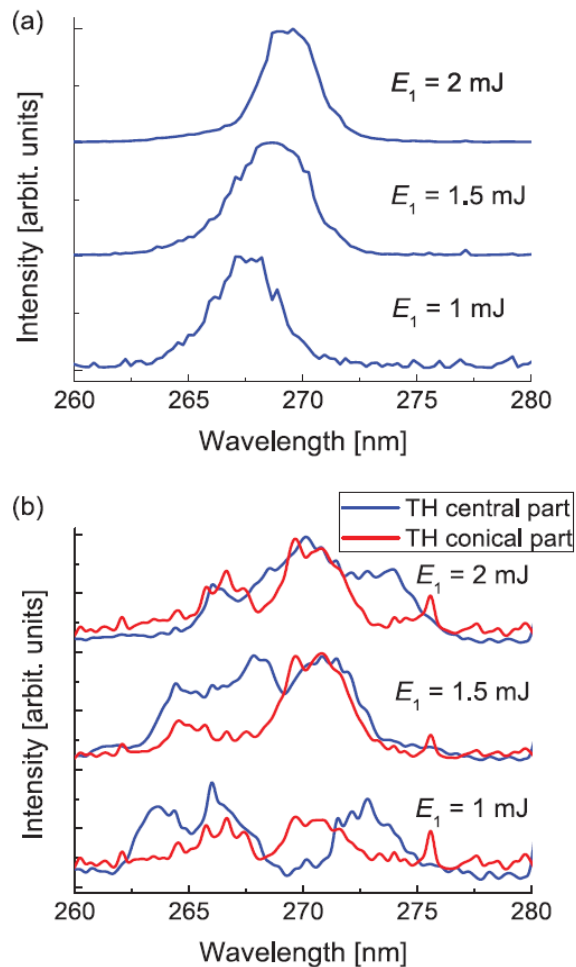


Fig. 2.2.8. (a) The experimentally registered TH spectra for different total pump pulse energies  $E_1$  in the case of (a) SWM and (b) direct THG (pulse duration 100 fs).

### 3. APPLICATIONS OF NONCOLLINEAR SIX-WAVE MIXING FOR TEMPORAL CHARACTERIZATION OF FEMTOSECOND LASER PULSES

The simplest approach, which has been used for a long time to estimate laser pulse duration and other temporal characteristics, is that of second-order intensity autocorrelation measurements. Though this method allows a credible estimation of the

pulse duration, the second-order autocorrelation trace is always symmetric, regardless of the test-pulse symmetry, i.e., it cannot resolve the time ambiguity. In addition, second harmonic autocorrelation measurements require broadband phase matching, which in the case of ultrashort pulses requires very thin nonlinear crystals [82-90]. In addition to second-order intensity autocorrelation measurements more sophisticated methods of determining the pulse shape from higher-order autocorrelation functions, using THG [91, 92] or four-wave mixing and its combination with SH generation, are known [93, 94]. However, these methods are not yet widely used due to their complexity and cumbersome interpretation of the experimental data. It should be stressed in this context that the characterization of laser pulses scales well with the autocorrelation order, and, importantly, higher-order autocorrelations (apart from the pulse duration) may provide additional information about pulse asymmetry and substructure. In order to demonstrate the advantages of higher-order autocorrelations, the plots of a bimodal (having two bellshaped Gaussian intensity humps) test function together with its second-order (left panel) and fifth-order (right panel) autocorrelation functions, defined as

$$G^{(n)}(\tau) = \int_{-\infty}^{+\infty} I_L^{n-1}(t)I_L(t - \tau)dt, \quad (3.1)$$

with  $n = 2$  and  $n = 5$ , are plotted in Fig. 3.1. It is easy to notice that the fifth-order autocorrelation trace indeed shows the realistic temporal intensity of the pulse. (Note that straightforward evaluation shows that the width of the  $n$ th-order autocorrelation traces  $\tau_A$  scales as

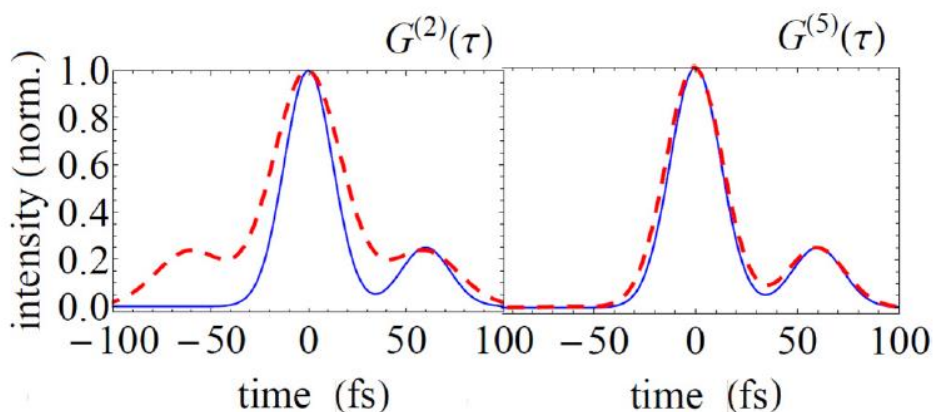


Fig. 3.1. Plots of a bimodal test function (solid lines) and corresponding second- and fifth-order intensity autocorrelation functions (dashed lines) on the left and right panels, respectively.



$$\tau_A = \sqrt{\frac{n}{n-1}} \tau_L, \quad (3.2)$$

compared with the width of the Gaussian pulse  $\tau_L$ ). Therefore, the main drawbacks of pulse characterization by second-order autocorrelations can be overcome by measuring the higher order autocorrelations.

Further, we consider the specific case of THG in two-beam pump geometry (shown in Fig. 3.2) that separates out the phase matched background-free TH signal fields with complex amplitudes  $\varepsilon_{TH}^{(1,2)}$  TH obtained through the SWM and direct THG signal (if any) in an instantaneous two-dimensional mapping.

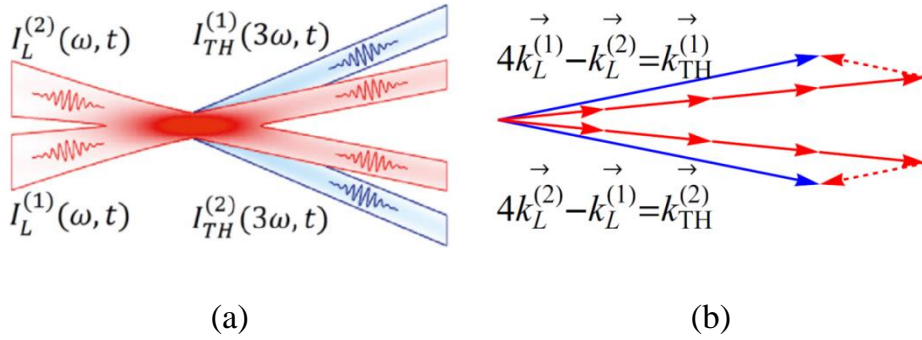


Fig. 3.2. (a) Configuration of the pump  $I_L(t)$  and THG  $I_{THG}(t)$  beams during phase-matched noncollinear SWM in air. (b) a wave-vector diagram of the same process.

Thus, in the absence of resonances, the SWM process can be interpreted as

$$\varepsilon_{TH} = \varepsilon_{TH}^{(1)} + \varepsilon_{TH}^{(2)} \sim \chi^{(5)} (\varepsilon_L^{(1)4} \varepsilon_L^{(2)*} + \varepsilon_L^{(2)4} \varepsilon_L^{(1)*}), \quad (3.3)$$

where  $\varepsilon_L^{(1,2)}$  denotes the complex amplitudes of the fundamental field in different pump beams, and  $\chi^{(5)}$  is the nonresonant fifth-order nonlinear susceptibility. In our SWM geometry, light-matter interaction at the fundamental frequency  $\omega$  produces a third harmonic signal at frequency  $\omega_{TH} = 4\omega^{(1,2)} - \omega^{(1,2)}$ , where the superscripts 1 and 2 indicate that the fields from different pump beams are involved. Since during our experiments the signal energy at the TH frequency is measured in one of the generation channels, a variation in the time delay  $\tau$  between two pump pulses gives a signal  $|\varepsilon_{TH}^{(1)}|^2$  in the form of a fifth-order intensity autocorrelation function  $G^{(5)}(\tau)$  of the fundamental pulse. It should be remembered that in the wave-mixing process, a phase-matching bandwidth is defined by the function  $\text{sinc}(\Delta k L / 2)$ , where  $\Delta k$  is the phase mismatch

between the frequencies of the fundamental and TH pulses, and  $L$  stands for the interaction length. Note that due to the low air dispersion and small interaction angles necessary for efficient SWM, extremely broad phase-matching bandwidths (FWHM) can be obtained (see Fig. 3.3), which under typical experimental conditions (central laser wavelength of 800 nm,  $L \approx 1$  cm) are about 340 nm and support pulse duration measurements as short as 5 fs.

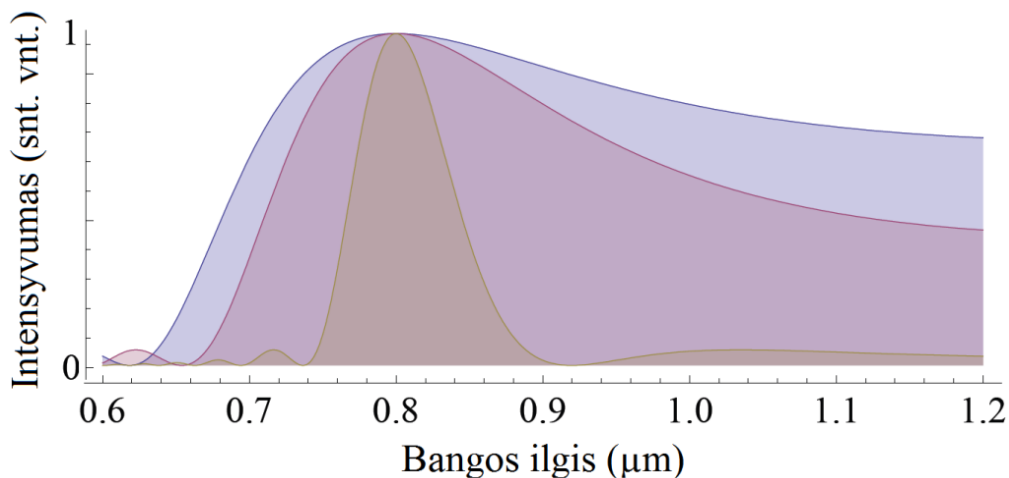


Fig. 3.3. The phase-matching bandwidth shapes for SWM in air, when interaction length is: 4 cm (the narrowest curve), 1.5 cm and 1 cm (the widest curve).

An optical delay line inserted into the path of one of the beams allowed us to vary the time delay  $\tau$  between the two pump pulses (Fig. 2.1.1) and to register their fifth-order autocorrelation. In addition, in order to monitor the duration of laser pulses, we also used a noncollinear second harmonic (SH) autocorrelator. The SH autocorrelations were recorded by placing a thin beta barium borate (BBO) crystal in the beam crossing region and varying the time delay  $\tau$  between the pulses.

Experimentally recorded  $G^{(5)}(\tau)$  traces are presented in Fig. 3.4 (black squares). It can be seen that for the total FH energy of 0.6 mJ, the autocorrelation trace (Fig. 3.4 (a)) remains practically symmetric above level  $10^{-1}$  from the maximum of the pulse amplitude. However, the second satellite spike at the  $10^{-2}$  level in the trailing part can

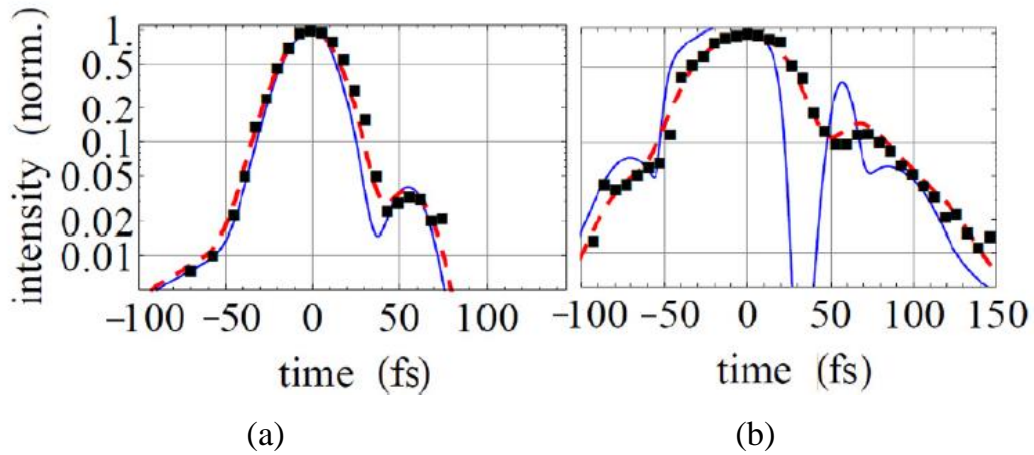


Fig. 3.4. Black squares: logarithmic plots of experimentally measured (using SWM in air) fifth-order autocorrelations from (a) 0.6 mJ and (b) 0.8 mJ pump pulses with 35 fs durations. The solid line marks the recovered intensity of the pulse obtained by fitting its fifth-order correlation function (dashed line) to the experimental data.

easily be seen, which indicates that under given experimental conditions the early stages of beam filamentation are already taking place. This assumption is confirmed further by studying the experimentally recorded autocorrelation traces for the 0.8 mJ total pump pulse energy (Fig. 3.4 (b)). In this case, one can observe flattening of the main peak as well as splitting (formation of subpulses in the trailing and leading parts) of the laser pulse. A subpulse with a duration as short as 10 fs in the trailing part of the pulse (blue solid line) was observed by fitting its fifth-order correlation function (red dashed line) to experimental data, and this fact further supports our prediction that SWM is capable of characterizing extremely short pulses.

## CONCLUSIONS

1. The long filaments (up to 50 cm) and the large spectral shifts of the pump and generated third harmonic pulses (up to 20 nm and 50 nm, respectively) were observed, when the femtosecond pulses of Ti:sapphire laser were focused by the lenses of long focal length (2 m). It was found that these spectral shifts do not saturate, but grow linearly with the pump pulse energy (up to 3 mJ) and are proportional to the filament length, which is also linearly dependent on the pump pulse energy. These spectral shifts grow due to the increased filament length, which increases the high intensity area where the plasma generation, self-phase modulation and cross-phase modulation, i.e., the effects inducing spectral shifts to the interacting light pulses are taking place.

2. It was shown experimentally and theoretically that by focusing the femtosecond laser pulses by the lenses of long focal length ( $\sim 2$  m) and increasing pump pulse energy the additional filament can be formed where the strong spectral blue-shift of the third harmonic axial part is taking place. This spectral shift is caused by the plasma electrons generated in the additional filament. Meanwhile, the conical part of the third harmonic radiation is generated in the first filament and due to the off-axis propagation does not interact with the plasma electrons of the second filament, therefore its spectrum does not change considerably during the refocusing.

3. The phase-matched frequency tripling due to the noncollinear six-wave mixing with phase-matching controlled via a change of the pump beam crossing angle in air was demonstrated for the first time both experimentally and theoretically. It was shown that this process is the most efficient (the maximal energy conversion efficiency reaches  $10^{-4}$ ), when two pump beams are crossed at the phase-matching angle of the six-wave mixing (13 mrad).

4. It was demonstrated that during noncollinear six-wave mixing of the femtosecond laser pulses in air the most of the generated third harmonic pulse energy can be concentrated into a single Gaussian beam. Since the third harmonic photon is generated when four photons from one pump beam are interacting with one photon from the other beam, maximal conversion efficiency is achieved, when the pump beam intensity ratio is

1:4 or 4:1. Under the conditions of this pump beam intensity ratio the additional increase of third harmonic conversion efficiency (up to 25%) was obtained, compared with the case of equal intensity pump beams.

5. It was demonstrated that the signal of noncollinear six-wave mixing obtained by varying time delay between the two pump pulses is proportional to the fifth-order autocorrelation function of these pulses, which allows not only to determine the duration of the investigated pulses, but also provides the information about the temporal pulse form and possible its asymmetry. It was shown theoretically that this technique allows the temporal characterization of the laser pulses having durations shorter than 5 fs because due to the low air dispersion the extremely broad phase-matching bandwidth (340 nm) of six-wave mixing is taking place. It was demonstrated experimentally that this nonlinear phenomenon can be used also for the registration of the six-wave mixing FROG traces of the femtosecond laser pulses.

## BIBLIOGRAPHY

- [1] F. Théberge, N. Aközbek, W. Liu, J.-F. Gravel, and S. L. Chin, Third harmonic beam profile generated in atmospheric air using femtosecond laser pulses, *Opt. Commun.* **245**, 399-405 (2005).
- [2] F. Théberge, N. Aközbek, W. Liu, J. Filion, and S. L. Chin, Conical emission and induced frequency shift of third-harmonic generation during ultrashort laser filamentation in air, *Opt. Commun.* **276**, 298-304 (2007).
- [3] S. Backus, J. Peatross, Z. Zeek, A. Rundquist, G. Taft, M. M. Murnane, and H. C. Kapteyn, 16-fs, 1- $\mu$ J ultraviolet pulses generated by third-harmonic conversion in air, *Opt. Lett.* **21**, 665-667 (1996).
- [4] N. Aközbek, A. Iwasaki, A. Becker, M. Scalora, S. L. Chin, and C. M. Bowden, Third-Harmonic Generation and Self-Channeling in Air Using High-Power Femtosecond Laser Pulses, *Phys. Rev. Lett.* **89**, 143901 (2002).
- [5] F. Théberge, Q. Luo, W. Liu, S. A. Hosseini, M. Sharifi, and S. L. Chin, Long-range third-harmonic generation in air using ultrashort intense laser pulses, *Appl. Phys. Lett.* **87**, 081108 (2005).
- [6] L. Bergé, S. Skupin, G. Mejean, J. Kasparian, J. Yu, S. Frey, E. Salmon, and J. P. Wolf, Supercontinuum emission and enhanced self-guiding of infrared femtosecond filaments sustained by third-harmonic generation in air, *Phys. Rev. E* **71**, 016602 (2005).
- [7] X. Ting-Ting, Z. Jie, L. Xin, H. Zuo-Qiang, Y. Hui, D. Quan-Li, and W. Hui-Chun, Generation of third harmonic emission in propagation of femtosecond laser pulses in air, *Chin. Phys.* **15**, 2025–2029 (2006).
- [8] R. L. Sutherland, *Handbook of Nonlinear Optics* (Marcel Dekker, New York, 1996).
- [9] J. F. Reintjes, *Nonlinear Optical Parametric Processes in Liquids and Gases* (Academic Press, New York, 1984).

- [10] J. Reintjes, Frequency mixing in the extreme ultraviolet, *Appl. Opt.* **19**, 3889-3896 (1980).
- [11] J. F. Ward, and G. H. C. New, Optical Third Harmonic Generation in Gases by a Focused Laser Beam, *Phys. Rev.* **185**, 57-73 (1969).
- [12] C. Rodriguez, Z. Sun, Z. Wang, and W. Rudolph, Characterization of laser-induced air plasmas by third harmonic generation, *Opt. Express* **19**, 16115-16125 (2011).
- [13] P. J. Ding, Z. Y. Liu, Y. C. Shi, S. H. Sun, X. L. Liu, X. S. Wang, Z. Q. Guo, Q. C. Liu, Y. H. Li, and B. T. Hu, Spectral characterization of third-order harmonic generation assisted by a two-dimensional plasma grating in air, *Phys. Rev. A* **87**, 043828 (2013).
- [14] D. Yelin, and Y. Silberberg, Laser scanning third-harmonic-generation microscopy in biology, *Opt. Express* **5**, 169-175 (1999).
- [15] N. Aközbek, A. Becker, M. Scalora, S.L. Chin, and C.M. Bowden, Continuum generation of the third-harmonic pulse generated by an intense femtosecond IR laser pulse in air, *Appl. Phys. B* **77**, 177–183 (2003).
- [16] F. Théberge, W. Liu, Q. Luo, and S.L. Chin, Ultrabroadband continuum generated in air (down to 230 nm) using ultrashort and intense laser pulses, *Appl. Phys. B* **80**, 221–225 (2005).
- [17] R. W. Boyd, *Nonlinear Optics* (2nd ed., Academic Press, San Diego, CA, 2003).
- [18] D. Dietze, J. Darmo, S. Roither, A. Pugzlys, J. N. Heyman, and K. Unterrainer, Polarization of terahertz radiation from laser generated plasma filaments, *J. Opt. Soc. Am. B* **26**, 2016-2027 (2009).
- [19] D. Faccio, P. D. Trapani, S. Minardi, A. Bramati, F. Bragheri, C. Liberale, V. Degiorgio, A. Dubietis, and A. Matijosius, Far-field spectral characterization of conical emission and filamentation in Kerr media, *J. Opt. Soc. Am. B* **22**, 862-869 (2005).
- [20] E. T. J. Nibbering, P. F. Curley, G. Grillon, B. S. Prade, M. A. Franco, F. Salin, and A. Mysyrowicz, Conical emission from self-guided femtosecond pulses in air, *Opt. Lett.* **21**, 62-64 (1996).

- [21] O. G. Kosareva, V. P. Kandidov, A. Brodeur, C. Y. Chien, and S. L. Chin, Conical emission from laser–plasma interactions in the filamentation of powerful ultrashort laser pulses in air, *Opt. Lett.* **22**, 1332-1334 (1997).
- [22] V. Vaičaitis, Cherenkov-type phase-matched third harmonic generation in air, *Opt. Commun.* **185**, 197-202 (2000).
- [23] S. L. Chin, S. A. Hosseini, W. Liu, Q. Luo, F. Théberge, N. Aközbek, A. Becker, V. P. Kandidov, O. G. Kosareva, and H. Schroeder, The propagation of powerful femtosecond laser pulses in optical media physics, applications, and new challenges, *Can. J. Phys.* **83**, 863-905 (2005).
- [24] A. Couairon, and A. Mysyrowicz, Femtosecond filamentation in transparent media, *Phys. Rep.* **441**, 47– 189 (2007).
- [25] S. L. Chin, T. -J. Wang, C. Marceau, J. Wu, J. S. Liu, O. Kosareva, N. Panov, Y. P. Chen, J. -F. Daigle, S. Yuan, A. Azarm, W. W. Liu, T. Seideman, H. P. Zeng, M. Richardson, R. Li, and Z. Z. Xu, *Advances in Intense Femtosecond Laser Filamentation in Air*, *Las. Phys.* **22**, 1–53 (2012).
- [26] S. L. Chin, *Femtosecond laser filamentation* (Springer, New York, 2010).
- [27] A. Braun, G. Korn, G. Liu, X. Du, J. Squier, and G. Mourou, Self-channeling of high- peak-power femtosecond laser pulses in air, *Opt. Lett.* **20**, 73-75 (1995).
- [28] A. Penzkofer, and H. J. Lehmeier, Theoretical investigation of noncollinear phase-matched parametric four-photon amplification of ultrashort light pulses in isotropic media, *Opt. and Quant. Electr.* **25**, 815-844 (1993).
- [29] T. Fuji, T. Horio, and T. Suzuki, Generation of 12 fs deep-ultraviolet pulses by four-wave mixing through filamentation in Neon Gas, *Opt. Lett.* **32**, 2481-2483 (2007).
- [30] T. Fuji, and T. Suzuki, Generation of sub-two-cycle mid-infrared pulses by four-wave mixing through filamentation in air, *Opt. Lett.* **32**, 3330-3332 (2007).
- [31] F. Théberge, N. Aközbek, W. Liu, A. Becker, and S. L. Chin, *Tunable Ultrashort Laser Pulses Generated through Filamentation in Gases* (2006).



- [32] C. G. Durfee, S. Backus, H. C. Kapteyn, and M. M. Murnane, Intense 8-fs pulse generation in the deep ultraviolet, *Opt. Lett.* **24**, 697-699 (1999).
- [33] M. Beutler, M. Ghotbi, F. Noack, and I. V. Hertel, Generation of sub-50-fs vacuum ultraviolet pulses by four-wave mixing in argon, *Opt. Lett.* **35**, 1491-1493 (2010).
- [34] P. Zuo, T. Fuji, and T. Suzuki, Spectral phase transfer to ultrashort UV pulses through four-wave mixing, *Opt. Expr.* **18**, 16183-16192 (2010).
- [35] M. Ghotbi, P. Trabs, M. Beutler, and F. Noack, Generation of tunable sub-45 femtosecond pulses by noncollinear four-wave mixing, *Opt. Lett.* **38**, 486-488 (2013).
- [36] F. Munhoz, H. Rigneault, and S. Brasselet, Polarization-resolved four-wave mixing microscopy for structural imaging in thick tissues, *J. Opt. Soc. Am. B* **29**, 1541-1550 (2012).
- [37] A. M. Zheltikov, and N. I. Koroteev, Coherent four-wave mixing in excited and ionized gas media, *Phys. Uspekhi* **42**, 321-351 (1999).
- [38] S. Tzortzakis, L. Bergé, A. Couairon, M. Franco, B. Prade, and A. Mysyrowicz, Breakup and Fusion of Self-Guided Femtosecond Light Pulses in Air, *Phys. Rev. Lett.* **86**, 5470-5473 (2001).
- [39] G. Bjorklund, Effects of focusing on third-order nonlinear processes in isotropic media, *IEEE J. Quantum Electron.* **11**, 287-296 (1975).
- [40] Y. Liu, M. Durand, A. Houard, B. Forestier, A. Couairon, and A. Mysyrowicz, Efficient generation of third harmonic radiation in air filaments: A revisit, *Opt. Commun.* **284**, 4706-4713 (2011).
- [41] J. K. Wahlstrand, Y.-H. Cheng, Y.-H. Chen, and H. M. Milchberg, Optical Nonlinearity in Ar and N<sub>2</sub> near the Ionization Threshold, *Phys. Rev. Lett.* **107**, 103901 (2011).
- [42] A. Becker, N. Aközbek, K. Vijayalakshmi, E. Oral, C. Bowden, and S. Chin, Intensity clamping and re-focusing of intense femtosecond laser pulses in nitrogen molecular gas, *Appl. Phys. B* **73**, 287-290 (2001).

- [43] J. Kasparian, R. Sauerbrey, and S.L. Chin, The critical laser intensity of self-guided light filaments in air, *Appl. Phys. B*, **71**, 877–879 (2000).
- [44] W. Liu, S. Petit, A. Becker, N. Aközbek, C. M. Bowden, and S. L. Chin, Intensity clamping of a femtosecond laser pulse in condensed matter, *Opt. Commun.* **202**, 189-197 (2002).
- [45] A. B. Fedotov, N. I. Koroteev, M. M. T. Loy, X. Xiao, and A. M. Zheltikov, Saturation of third-harmonic generation in a plasma of self-induced optical breakdown due to the self-action of 80-fs light pulses, *Opt. Commun.* **133**, 587–595 (1997).
- [46] C.-J. Zhu, Y.-D. Qin, H. Yang, S.-F. Wang, and Q.-H. Gong, Third-order harmonic generation in atmospheric air with focused intense femtosecond laser pulses, *Chin. Phys. Lett.* **18**, 57–59 (2001).
- [47] H. Yang, J. Zhang, J. Zhang, L.Z. Zhao, Y.J. Li, H. Teng, Y.T. Li, Z.H. Wang, Z.L. Chen, Z.Y. Wei, J.X. Ma, W. Yu, and Z.M. Sheng, Third-order harmonic generation by self-guided femtosecond pulses in air, *Phys. Rev. E*, **67**(1), 015401-1–015401-4 (2003).
- [48] J. Peatross, S. Backus, J. Zhou, M. M. Murnane, and H. C. Kapteyn, Spectral-spatial measurements of fundamental and third-harmonic light of intense 25-fs laser pulses focused in a gas cell, *J. Opt. Soc. Am. B*, **15**(1), 186–192 (1998).
- [49] N. Aközbek, A. Becker, M. Scalora, S. L. Chin, and C. M. Bowden, Intensity clamping of a femtosecond laser pulse in condensed matter, *Appl. Phys. B* **77**, 177-197 (2003).
- [50] J. Bethge, C. Bree, H. Redlin, G. Stibenz, P. Staudt, G. Steinmeyer, A. Demircan, and S. Dusterer, Self-compression of 120 fs pulses in a white-light filament, *J. Opt.* **13**, 055203 (2011).
- [51] M. Mlejnek, E. M. Wright, and J. V. Moloney, Dynamic spatial replenishment of femtosecond pulses propagating in air, *Opt. Lett.* **23**, 382–384 (1998).
- [52] A. Talebpour, S. Petit, and S. L. Chin, Re-focusing during the propagation of a focused femtosecond Ti:sapphire laser pulse in air, *Opt. Commun.* **171**, 285-290 (1999).

- [53] B. M. Penetrante, J. N. Bardsley, W. M. Wood, C. W. Siders, and M. C. Downer, Ionization-induced frequency shifts in intense femtosecond laser pulses, *J. Opt. Soc. Am. B* **9**, 2032-2040 (1992).
- [54] G. Marcus, A. Zigler, and Z. Henis, Third-harmonic generation at atmospheric pressure in methane by use of intense femtosecond pulses in the tight-focusing limit, *J. Opt. Soc. Am. B* **16**, 792-800 (1999).
- [55] E. Yablonovitch, Energy conservation in the picosecond and subpicosecond photoelectric effect, *Phys. Rev. Lett.* **60**, 795-796 (1988).
- [56] B. C. Stuart, M. D. Feit, S. Herman, A. M. Rubenchik, B. W. Shore, and M. D. Perry, Nanosecond-to-femtosecond laser-induced breakdown in dielectrics, *Phys. Rev. B* **53**, 1749-1791 (1996).
- [57] C. W. Siders, N. C. Turner III, and M. C. Downer, Blue-shifted third-harmonic generation and correlated self-guiding during ultrafast barrier suppression ionization of subatmospheric density noble gases, *J. Opt. Soc. Am. B* **13**, 330-335 (1996).
- [58] E. V. Vanin, A. V. Kim, M. C. Downer, and A. M. Sergeev, Excitation of ultrashort burst of the radiation during ionization of a gas by an intense light pulse, *JETP Lett.* **58**, 900-906 (1993).
- [59] V. B. Gil'denburg, V. I. Pozdnyakova, and I. A. Shereshevskii, Frequency self-upshifting of focused electromagnetic pulse producing gas ionization, *Phys. Lett. A* **203**, 214-218 (1995).
- [60] E. T. J. Nibbering, M. A. Franco, B. S. Prade, G. Grillon, J.-P. Chambaret, and A. Mysyrowicz, Spectral determination of the amplitude and the phase of intense ultrashort optical pulses, *J. Opt. Soc. Am. B* **13**, 317-329 (1996).
- [61] X. Liu, X. Lu, X. Liu, L. Feng, J. Ma, Y. Li, L. Chen, Q. Dong, W. Wang, Z. Wang, Z. Wei, Z. Sheng, and J. Zhang, Broadband supercontinuum generation in air using tightly focused femtosecond laser pulses, *Opt. Lett.* **36**, 3900-3902 (2011).
- [62] N. I. Koroteev, and A. M. Zheltikov, Cross-phase-modulation-controlled third-harmonic generation in gases, *Las. Phys.* **8**, 512-517 (1998).

- [63] J. W. Wilson, P. Samineni, W. S. Warren, and M. C. Fischer, Cross-phase modulation spectral shifting: nonlinear phase contrast in a pump-probe microscope, *Biomed. Opt. Express* **3**, 854-862 (2012).
- [64] F. De Martini, C. H. Townes, T. K. Gustapson, and P. L. Kelley, Self-Steepening of Light Pulses, *Phys. Rev.* **164**, 312-323 (1967).
- [65] G. Yang, and Y. R. Shen, Spectral broadening of ultrashort pulses in a nonlinear medium, *Opt. Lett.* **9**, 510-512 (1984).
- [66] A. Brodeur, and S. L. Chin, Ultrafast white-light continuum generation and self-focusing in transparent condensed media, *J. Opt. Soc. Am. B* **16**, 637-650 (1999).
- [67] M. Kolesik, E. M. Wright, A. Becker, and J. V. Moloney, Simulation of third-harmonic and supercontinuum generation for femtosecond pulses in air, *Appl. Phys. B* **85**, 531–538 (2006).
- [68] J. E. Rothenberg, Space-time focusing breakdown of the slowly varying envelope approximation in the self-focusing of femtosecond pulses, *Opt. Lett.* **17**, 1340-1342 (1992).
- [69] A. L. Gaeta, Catastrophic Collapse of Ultrashort Pulses, *Phys. Rev. Lett.* **84**, 3582-3585 (2000).
- [70] N. Aközbek, M. Scalora, C.M. Bowden, and S. L. Chin, White-light continuum generation and filamentation during the propagation of ultrashort laser pulses in the air, *Opt. Commun.* **191**, 353-362 (2001).
- [71] V. Vaičaitis, V. Jarutis, and A. Stabinis, Transverse and longitudinal phase-matching in third harmonic generation induced by the Bessel beams, *Opt. Commun.* **284**, 3101–3104 (2011).
- [72] S. E. Harris, Generation of Vacuum-Ultraviolet and Soft—X-Ray Radiation Using High-Order Nonlinear Optical Polarizabilities, *Phys. Rev. Lett.* **31**, 341-344 (1973).

- [73] J. Reintjes, C.-Y. She, and R. C. Eckardt, Generation of coherent radiation in XUV by fifth- and seventh-order frequency conversion in rare gases, *IEEE J. Quantum Electron.* **14**, 581-596 (1978).
- [74] K. Kosma, S. A. Trushin, and W. E. Schmid, W. Fuß, Vacuum ultraviolet pulses of 11 fs from fifth-harmonic generation of a Ti:sapphire laser, *Opt. Lett.* **33**, 723-725 (1996).
- [75] V. Vaičaitis, V. Jarutis, and D. Pentaris, Conical Third-Harmonic Generation in Normally Dispersive Media, *Phys. Rev. Lett.* **103**, 103901 (2009).
- [76] J. B. Bertrand, H. J. Worner, H.-C. Bandulet, E. Bisson, M. Spanner, J.-C. Kieffer, D. M. Villeneuve, and P. B. Corkum, Ultrahigh-Order Wave Mixing in Noncollinear High Harmonic Generation, *Phys. Rev. Lett.* **106**, 023001 (2011).
- [77] K. Hartinger, and R. A. Bartels, Enhancement of third harmonic generation by a laser-induced plasma, *Appl. Phys. Lett.* **93**, 151102 (2008).
- [78] X. Yang, J. Wu, Y. Peng, Y. Tong, S. Yuan, L. Ding, Z. Xu, and H. Zeng, *Appl. Phys. Lett.* **95**, 111103 (2009).
- [79] S. Suntsov, D. Abdollahpour, D. G. Papazoglou, and S. Tzortzakis, Efficient third-harmonic generation through tailored IR femtosecond laser pulse filamentation in air, *Opt. Express* **17**, 3190-3195 (2009).
- [80] S. Suntsov, D. Abdollahpour, D. G. Papazoglou, and S. Tzortzakis, Filamentation-induced third-harmonic generation in air via plasma-enhanced third-order susceptibility, *Phys. Rev. A* **81**, 033817 (2010).
- [81] V. E. Peet, and R. V. Tsubin, Gas-phase generation of resonance-enhanced third harmonic with crossed laser beams, *Opt. Commun.* **214**, 381-387 (2002).
- [82] D. Meshulach, Y. Barad, and Y. Silberberg, Measurement of ultrashort optical pulses by third-harmonic generation, *J. Opt. Soc. Am. B* **14**, 2122-2125 (1997).
- [83] D. J. Bradley, and G. H. C. New, Ultrashort pulse measurements *Proc, IEEE* **62**, 313-345 (1974).

- [84] M. Nisoli, S. D. Silvestri, O. Svelto, R. Szipocs, K. Ferencz, C. Spielmann, S. Sartania, and F. Krausz, Compression of high-energy laser pulses below 5 fs, *Opt. Lett.* **22**, 522-524 (1997).
- [85] E. P. Ippen, and C. V. Shank, *Ultrashort Light Pulses: Picosecond Techniques and Applications* (Springer, Berlin, 1977).
- [86] R. N. Gyuzalian, S. B. Sogominian, and Z. G. Horvath, Background-free measurement of time behaviour of an individual picosecond laser pulse, *Opt. Commun.* **29**, 239-242 (1979).
- [87] P. Heinz, A. Reuther, and A. Laubereau, Additive-pulse modelocking of non-cw neodymium lasers, *Opt. Commun.* **97**, 35-40 (1993).
- [88] M. Maier, W. Kaiser, and J. A. Giordmaine, Intense Light Bursts in the Stimulated Raman Effect, *Phys. Rev. Lett.* **17**, 1275-1277 (1966).
- [89] R. Trebino, and D. J. Kane, *J. Opt. Soc. Am. A* **10**, 1101 (1993).
- [90] D. N. Fittinghoff, J. L. Bowie, J. N. Sweetser, R. T. Jennings, M. A. Krumbugel, K. W. DeLong, R. Trebino, and I. A. Walmsley, *Opt. Lett.* **21**, 12 (1996).
- [91] G. G. Grigoryan, A. O. Melikyan, D. G. Sarkisyan, and A. S. Sarkisyan, Determination of the third-order correlation function by noncollinear two-beam third-harmonic generation, *Quantum Electron.* **25**, 262-266 (1995).
- [92] T.-M. Liu, Y.-C. Huang, G.-W. Chern, K.-H. Lin, C.-J. Lee, Y.-C. Hung, and C.-K. Sun, Triple-optical autocorrelation for direct optical pulse-shape measurement, *Appl. Phys. Lett.* **81**, 1402-1404 (2002).
- [93] D. Meshulach, Y. Barad, and Y. Silberberg, Measurement of ultrashort optical pulses by third-harmonic generation, *J. Opt. Soc. Am. B* **14**, 2122-2125 (1997).
- [94] N. A. Papadogiannis, S. D. Moustazis, P. A. Loukakos, and C. Kalpouzos, Temporal characterization of ultra short laser pulses based on multiple harmonic generation on a gold surface, *Appl. Phys. B* **65**, 339-345 (1997).

## SANTRAUKA

### FEMTOSEKUNDINIŲ LAZERIO IMPULSŲ TREČIOSIOS HARMONIKOS GENERAVIMAS IR ŠEŠIABANGIS DAŽNIŲ MAIŠYMAS ORE

Disertacijos darbo tikslas buvo ištirti trečiosios harmonikos spektrines savybes ir jų pokyčius pluošto refokusavimosi metu bei pademonstruoti trečiosios harmonikos generaciją dėl šešiabangio dažnių maišymo, tuo pačiu analizuojant šio reiškinio charakteristikas (erdvines, spektrines, energines) bei taikymų galimybes, ore naudojant femtosekundinius impulsus.

Parodyta, kad, Ti:Safyro lazerio femtosekundinius impulsus fokusuojant ilgo židinio nuotolio lęšiais (1-2 m), pasireiškia dideli žadinimo ir ore generuojamos trečiosios harmonikos spektriniai poslinkiai (atitinkamai 50 nm ir 20 nm). Eksperimentiškai ir skaitmeniškai parodyta, kad dėl pluošto refokusavimosi gali formuotis trūkios šviesos gijos, kuriose padidėja pirmosios ir trečiosios harmonikų spektriniai poslinkiai.

Taip pat disertacijoje pirmą kartą pademonstruotas efektyvus dažnio trigubinimas ore, naudojant nekolinearaus šešiabangio dažnių maišymo reiškinį, kurio fazinio sinchronizmo sąlygos kontroliuojamos, keičiant žadinimo pluoštų susikirtimo kampą. Be to, naudojant dviejų žadinimo pluoštų konfigūraciją, optimizuotos energinės ir erdvinės trečiosios harmonikos, generuojamos nekolinearaus šešiabangio dažnių maišymo ore metu, charakteristikos. Pademonstruota, kad, keičiant dviejų žadinimo pluoštų intensyvumų santykį, galima beveik visą generuojamos trečiosios harmonikos energiją iš dviejų trečiosios harmonikos pluoštų perduoti į vieną Gauso formos pluoštą. Maksimalus energijos perdavimas į vieną pluoštą gautas, kai žadinimo pluoštų intensyvumų santykis buvo 1:4 arba 4:1. Be to, pademonstruota, kad nekolinearus šešiabangis dažnių maišymas gali būti naudojamas galingų femtosekundinių lazerio impulsų charakterizavimui, t. y. jų penktosios eiles autokoreliacinių funkcijų registravimui. Maža oro dispersija trečiosios harmonikos signalą leidžia vienu metu generuoti plačiame žadinimo impulsų spektriniame diapazone (apie 340 nm), o tai atitinka mažesnę nei 5 fs charakterizuojamų impulsų trukmę.

## CURRICULUM VITAE

Name	Kęstutis
Surname	Steponkevičius
E-mail	kestutis.steponkevicius@ff.vu.lt
Place of birth	Varėna
Date of birth	1986.11.21
Nationality	Lithuanian

### Education:

1994–2006	Vilnius Fabijoniškių Secondary School
2006–2010	Vilnius University, Faculty of Physics. Bachelor degree.
2010–2012	Vilnius University, Faculty of Physics. Master degree.
2012–2016	Vilnius University, Faculty of Physics, Department of Quantum Electronics. PhD studies.

### Work experience:

2012.10 – 2015.09	VU LTC (junior research fellow)
2011.07 – 2012.09	VU LTC (engineer)